Smart Structures and Systems, Vol. 6, No. 7 (2010) 767-792
DOI: http://dx.doi.org/10.12989/sss.2010.6.7.767

Semi-analytical solutions for optimal distributions of sensors and actuators in smart structure vibration control

Zhanli Jin[1], Yaowen Yang*[2] and Chee Kiong Soh[2]

[1]*School of Electrical and Electronics Engineering, Nanyang Technological University (NTU), Singapore 639798*
[2]*School of Civil and Environmental Engineering, Nanyang Technological University (NTU), Singapore 639798*

(Received August 27, 2008, Accepted October 8, 2009)

Abstract. In this paper, the optimal design of vibration control system for smart structures has been investigated semi-analytically via the optimization of geometric parameters like the placements and sizes of piezoelectric sensors and actuators (S/As) bonded on the structures. The criterion based on the maximization of energy dissipation was adopted for the optimization of the control system. Based on the sensing and actuating equations, the total energy stored in the system which is used as the objective function was analytically derived with design variables explicitly presented. Two cases of single and combined vibration modes were addressed for a simply supported beam and a simply supported cylindrical shell. For single vibration mode, the optimal distributions of the piezoelectric S/As could be obtained analytically. However, the Sequential Quadratic Programming (SQP) method has to be employed to solve those which violated the prescribed constraints and to solve the case of combined vibration modes. The results of three examples, which include a simply supported beam, a simply supported cylindrical shell and a simply supported plate, showed good agreement with those obtained by the Genetic Algorithm (GA) method. Moreover, in comparison with the GA method, the proposed method is more effective in obtaining better optimization results and is much more efficient in terms of computation time.

Keywords: optimization; vibration control; sequential quadratic programming; smart structures.

1. Introduction

In recent years, smart structures for vibration control of flexible space structures have attracted considerable amount of research. Piezoelectric materials as distributed sensors and actuators (S/As) have been applied in structural vibration control to take advantage of their fast broadband frequency responses and their flexibility to be used as S/As in a large variety of applications. The smart structure, which contains the main structure and the distributed piezoelectric S/As, can sense the excitations induced by its environment and can also generate control forces to eliminate the undesirable effects or to enhance the desirable effects. Application of smart structures to vibration control may be traced to Bailey and Hubbard (1985). There were also other researchers (Arockiasamy *et al*. 1992, Chandrashekhara and Agarwal 1993, Kalaycioglu *et al*. 1998) who have done a great deal of study on this issue. To ensure maximum control effectiveness, the piezoelectric S/As have to be of suitable size and be appropriately located which result in challenges for optimal vibration control.

*Corresponding Author, Associate Professor, E-mail: cywyang@ntu.edu.sg

The issues of S/A location and geometry, and their optimal selections with respect to certain performance criteria have drawn much attention due to their importance in structural sensing and control. Crawley and de Luis (1987) were the first to address the criterion for finding the optimal location of a piezoelectric actuator for a cantilever beam. Baz and Poh (1988) solved the problem of location optimization of a preselected actuator size. Devasia *et al*. (1993) considered the problem of placement and sizing optimization of distributed piezoelectric actuators in a uniform beam. Udwadia (1994) proposed a methodology for optimally locating sensors in a vibrating system for best identification of the parameters to be identified. Generally, the optimization methods for these issues fall into two categories: traditional methods and genetic-based methods. Kondoh *et al*. (1990) investigated the determination of sensor and actuator positioning and feedback gains for the active vibration control of flexible structures using a recursive quadratic programming algorithm. Lee and Chen (1994) developed a method for the determination of actuator/sensor locations and feedback gain via minimization of an energy criterion with a quasi-Newton or recursive quadratic programming algorithm. Varadan *et al*. (1997) adopted a gradient-based method to study the optimal placement and size of disk-shaped piezoelectric actuators to reduce the radiated sound. Bruant *et al.* (2001) proposed a new approach to find the optimal location of piezoelectric actuators and sensors on beam structures. The method was based on the differentiation of the optimization criteria and equations of motion with respect to the design variables. However, all these conventional optimization techniques encountered difficulties in dealing with piezoelectric patches confined to discrete locations.

Recently, genetic algorithm (GA) as an optimization technique has been applied to this kind of optimization problems. Krishnakumar and Goldberg (1992) explored the use of GA to solve aerospace-related control system optimization problems. Lee and Han (1996) used GA to obtain the piezoelectric actuator configuration which maximized the degrees of controllability. Zhang *et al*. (2000) presented a float-encoded GA for the optimal control of flexible smart structures bonded with piezoelectric S/As. Yang *et al*. (2005, 2006) developed a modified GA to simultaneously optimize the parameters of vibration control system of smart structures, including the placement and size of piezoelectric S/As bonded on smart structures and the feedback control gains. These GA-based optimization methods have the advantage of finding the global optimum robustly instead of being easily trapped in the local optimum. Jin *et al*. (2005) proposed a fuzzy GA system for optimal vibration control of smart cylindrical shells, which improved the search efficiency as compared to the standard GA.

Both the conventional and the GA methods are essentially numerical computation methods which involve a sequence of iteration processes. As an alternate counterpart, the analytical computation method can also be employed for the optimization with the advantage of avoiding iteration and finding the solutions directly and quickly. However, for those problems with more design variables or implicit objective function expressions, the analytical computation method will encounter difficulties in finding the optimization solutions. For such problems, the semi-analytical method which combines the analytical and numerical methods is able to improve the computation speed as partial analytical solutions are used. Wang and Quek (2002) proposed a basic mechanics model for the flexural analysis of beams with embedded piezoelectric layers and carried out a semi-analytical analysis for the dynamic characteristics of the entire structure. Yang *et al*. (2003) took into account the effect of axial load for the vibration control of a cantilever column based on analytical and semi-analytical solutions. Qing *et al*. (2006) presented a semi-analytical solution for the static and dynamic analysis of a clamped aluminum plate with piezoelectric patches.

In this study, the optimal design of vibration control system for smart structures was investigated

semi-analytically with the placements and sizes of piezoelectric S/As as design parameters. The objective function which is the total energy stored in the system was derived analytically with design variables explicitly shown, and then used for the analytical solutions of the case of single vibration mode and the semi-analytical solutions of the case of combined vibration modes. The Sequential Quadratic Programming (SQP) method was employed for solving the latter case and those violating the prescribed constraints in the former case. The results obtained for a simply supported beam, a simply supported cylindrical shell and a simply supported plate showed good agreement with those obtained by the GA method. The proposed method was also more effective in obtaining better optimization results and much more efficient in terms of computation time.

2. Vibration control modeling and optimization criteria

Consider a beam model and a thin cylindrical shell model, each with Np pairs of collocated piezoelectric patches bonded on their surfaces as discretely distributed S/As, as shown in Figs. 1 and 2. b, t_b and L_b are the width, thickness and length of the beam, respectively, x_{i1} and x_{i2} are the coordinates of the ith pair of collocated piezoelectric patches bonded on the beam, R, h, L and β^* are the radius, thickness, length and curvature angle of the cylindrical shell, respectively, and x_{i1}, x_{i2}, β_{i1} and β_{i2} are the coordinates of the ith pair of collocated piezoelectric patches bonded on the shell. The patches on the upper surface are the actuators and those on the lower surface are the sensors. Assume that the piezoelectric patches are much thinner than the host structures, and are perfectly bonded on the structure surfaces. The effects of the bonding material on the properties of the whole structure are neglected. The material properties, e.g., mass and stiffness, of the piezoelectric patches are negligible as compared to those of the main structure. Using the modal decomposition method and truncating the vibration modes at N, Yang *et al*. (2005, 2006) derived the sensing and actuating equations of the beam and shell structures with control systems. Note that for shell structures, the first $N=m\times n$ vibration modes are taken into account. Introducing state vector $\boldsymbol{\chi}=[\eta_1, \eta_2, \ldots, \eta_N, \dot{\eta}_1, \dot{\eta}_2, \ldots, \dot{\eta}_N]^T$, where $\eta_j(t)$ (j=1,2,...,N) are the modal participation factors of the transverse displacement, the sensing and vibration equations can be written in the following state-space form. This is with the assumption of proportional damping or Reighley damping so as to decouple the damping matrix.

$$\begin{cases} \dot{\boldsymbol{\chi}} = \overline{\boldsymbol{A}}\boldsymbol{\chi} + \overline{\boldsymbol{B}}\boldsymbol{\phi}_a \\ \boldsymbol{\phi}_s = \overline{\boldsymbol{C}}\boldsymbol{\chi} \end{cases} \tag{1}$$

where

$$\overline{\boldsymbol{A}} = \begin{bmatrix} \boldsymbol{0}_{N\times N} & \boldsymbol{I}_{N\times N} \\ -\boldsymbol{\Omega}^2 & -2\boldsymbol{\varsigma}\boldsymbol{\Omega} \end{bmatrix}, \ \overline{\boldsymbol{B}} = \begin{bmatrix} \boldsymbol{0}_{N\times Np} \\ \widetilde{\boldsymbol{B}} \end{bmatrix}, \ \overline{\boldsymbol{C}} = [\widetilde{\boldsymbol{C}} \ \ \boldsymbol{0}_{Np\times N}], \tag{2}$$

$$\widetilde{\boldsymbol{B}} = \begin{bmatrix} B_{11} & B_{12} & \cdots & B_{1Np} \\ B_{21} & B_{22} & \cdots & B_{2Np} \\ & & \vdots & \\ B_{N1} & B_{N2} & \cdots & B_{NNp} \end{bmatrix}, \ \boldsymbol{\phi}_a = \begin{bmatrix} \phi_1^a \\ \phi_2^a \\ \vdots \\ \phi_{Np}^a \end{bmatrix}, \tag{3}$$

$$\widetilde{\boldsymbol{C}} = \begin{bmatrix} C_{11} & C_{12} & & C_{1N} \\ C_{21} & C_{22} & \cdots & C_{2N} \\ \vdots & \vdots & & \vdots \\ C_{Np1} & C_{Np2} & & C_{NpN} \end{bmatrix}, \ \boldsymbol{\phi}_s = \begin{bmatrix} \phi_1^s \\ \phi_2^s \\ \vdots \\ \phi_{Np}^s \end{bmatrix}, \tag{4}$$

For beam structures, the coefficients in Eqs. (3) and (4) can be expressed as

$$B_{ji} = K_a[U_j'(x_{i2}) - U_j'(x_{i1})], \ C_{ij} = K_s[U_j'(x_{i2}) - U_j'(x_{i1})], \tag{5}$$

in which $U_j(x)$ are the mode shape functions of the transverse displacement, $K_a = br^a d_{31} E_p$, $K_s = -\dfrac{h^s}{x_{i2} - x_{i1}} h_{31} r^s$, $i = 1,2,..., Np$, and $j = 1,2,..., N$.

For shell structures, the coefficients in Eqs. (3) and (4) can be expressed as

$$B_{ji} = \frac{-e_{31}^a}{\rho h N_{pq}} \cdot \int_{\beta_{i1}}^{\beta_{i2}} \int_{x_{i1}}^{x_{i2}} [r^a (\frac{\partial^2 U_{pq}}{\partial x^2} + \frac{1}{R^2} \frac{\partial^2 U_{pq}}{\partial \beta^2}) - \frac{U_{pq}}{R}] R dx d\beta, \tag{6}$$

$$C_{ij} = \frac{h^s e_{31}^s}{S_i^e \varepsilon_{33}} \cdot \int_{\beta_{i1}}^{\beta_{i2}} \int_{x_{i1}}^{x_{i2}} [\frac{U_{pq}}{R} - r^s (\frac{\partial^2 U_{pq}}{\partial x^2} + \frac{\partial^2 U_{pq}}{R^2 \partial \beta^2})] R dx d\beta, \tag{7}$$

in which $U_{pq}(x, \beta)$ are the mode shape functions of the transverse displacement, $N_{pq} = \int_0^{\beta^*} \int_0^L U_{pq}^2 R dx d\beta$, $i = 1,2,..., Np$, $j = n \cdot (p\text{-}1) + q$, $p = 1,2,...,m$, $q = 1,2,...,n$.

$$\boldsymbol{\Omega} = \begin{bmatrix} \omega_1 & & & \\ & \omega_2 & & \\ & & \ddots & \\ & & & \omega_N \end{bmatrix}, \ \boldsymbol{\varsigma} = \begin{bmatrix} \varsigma_1 & & & \\ & \varsigma_2 & & \\ & & \ddots & \\ & & & \varsigma_N \end{bmatrix} \tag{8}$$

in which ω_j ($j = 1,2,...,N$) is the jth natural frequency of the structure, and ς_j is the damping ratio of the jth vibration mode. For shell structures, $\omega_j = \omega_{pq}$ ($j = n \cdot (p\text{-}1) + q$, $p = 1,2,...,m$, $q = 1,2,..., n$), and ω_{pq} is the natural frequency of the shell.

In the above equations, $\boldsymbol{\phi}_a$ is the voltage vector applied to the actuators and $\boldsymbol{\phi}_s$ is the output voltage vector over the sensors. For beam structures, d_{31} and E_p are the piezoelectric strain constant and the Young's modulus of the actuators, respectively, and h_{31} is the piezoelectric constant of the sensors. For shell structures, e_{31}^a and e_{31}^s are the piezoelectric stress constant of actuator and sensor, respectively, ε_{33} is the permittivity constant, and ρ is the mass density of the shell. In addition, h^s is the thickness of the sensor, r^s and r^a denote the distance measured from the neutral surface of the structure to the mid-surface of the sensor and actuator, respectively. For more details on the derivation of the state-space equations, refer to Yang *et al*. (2005, 2006).

The most attractive methodology that accounts for transient vibration responses is characterized by the maximization of the dissipation energy extracted by the feedback control system. The more the energy is dissipated by the control system, the less the energy is stored in the system. When considering a constant negative velocity feedback $\boldsymbol{\phi}_a = -\boldsymbol{G}\dot{\boldsymbol{\phi}}_s = -\boldsymbol{G}\overline{\boldsymbol{C}}\dot{\boldsymbol{\chi}}$, where $\boldsymbol{G}$ is the feedback gain matrix, the integrated total energy stored in the system can be written as

$$W = \int_0^\infty \chi^T \tilde{\boldsymbol{Q}} \chi dt \tag{9}$$

Application of the standard state transformation techniques to Eq. (9) yields

$$W = -\chi^T(t_0)\boldsymbol{P}\chi(t_0) \tag{10}$$

where $\chi(t_0)$ is the initial state and $\boldsymbol{P}$ is the solution of the following Lyapunov equation

$$\boldsymbol{A}^T\boldsymbol{P} + \boldsymbol{P}\boldsymbol{A} = \tilde{\boldsymbol{Q}} \tag{11}$$

in which

$$\boldsymbol{A} = \begin{bmatrix} \boldsymbol{0}_{N\times N} & \boldsymbol{I}_{N\times N} \\ -\Omega^2 & -\tilde{\boldsymbol{B}}\boldsymbol{G}\tilde{\boldsymbol{C}} - 2\varsigma\Omega \end{bmatrix}, \text{ and } \tilde{\boldsymbol{Q}} = \begin{bmatrix} \Omega^2 & \boldsymbol{0} \\ \boldsymbol{0} & \boldsymbol{I}_{N\times N} \end{bmatrix}.$$

Thus, the problem can be expressed as a nonlinear optimization problem with objective function W like

$$Minimize\ W(\vec{X}, Np) \tag{12}$$

where $\vec{X}$ is the vector of the coordinates of the S/As, which are defined as the design variables. The problem is also subject to geometric constraints to prevent overlapping any piezoelectric patches. For beam structures, $x_{i1} \le x_{i2}$ (i = 1,2,...,Np) and $x_{i2} \le x_{(i+1)1}$ (i = 1,2,...,Np-1) should be satisfied. For shell structures, the constraints of $x_{i1} \le x_{i2}$, $\beta_{i1} \le \beta_{i2}$, and $x_{j1} > x_{i2}$, or $x_{j2} < x_{i1}$, or $\beta_{j1} > \beta_{i2}$, or $\beta_{j2} < \beta_{i1}$ (i, j = 1,2,..., Np, $i \neq j$) are necessary.

It is worth noting that the optimization problem can be affected by the initial conditions. As reflected in Eq. (10), the initial conditions $\chi(t_0)$ are included in the objective function. This implies that different initial conditions have different objective functions, which affects the optimization results.

3. Analytical solution for single vibration mode

In this section, the optimal design of the control system for single vibration mode is discussed. In certain situations, if the structure is excited by some periodic external forces which have close or identical frequencies as the natural frequency of the structure, it is possible for the structure to vibrate in this specific frequency with a single mode. Thus, the control of this vibration mode is of main concern and the optimization of the geometric distribution of the S/As is important to achieve optimal control.

Assume that the jth vibration mode is considered and the feedback gain matrix is set as a constant g, the close-loop vibration equation with negative velocity feedback considered can be written as

$$\ddot{\eta}_j(t) + d \cdot \dot{\eta}_j(t) + \omega_j^2 \eta(t) = 0 \tag{13}$$

where

$$d = 2\zeta_j\omega_j + g \cdot \sum_{i=1}^{Np} B_{ji} \cdot C_{ij} \tag{14}$$

The solution of Eq. (13) can be expressed as follows if the initial conditions of $\eta_j(0) = 0$ and $\dot{\eta}_j(0) = v_j$ are assumed.

$$\eta_j(t) = \frac{v_j}{s_1 - s_2}(e^{s_1 t} - e^{s_2 t}) \tag{15}$$

where $$s_{1,2} = \frac{-d \pm \sqrt{d^2 - 4\omega_j^2}}{2}$$

Substituting Eq. (15) into Eq. (9), and noting that $d > 0$, the total energy stored in the system can be derived as

$$W = \int_0^\infty [\omega_j^2 \eta_j^2(t) + \dot{\eta}_j^2(t)]dt$$

$$= \int_o^\infty \left\{ \omega_j^2 \frac{v_j^2}{(s_1 - s_2)^2}[e^{2s_1 t} + e^{2s_2 t} - 2e^{(s_1 + s_2)t}] + \frac{v_j^2}{(s_1 - s_2)^2}[s_1^2 e^{2s_1 t} - 2s_1 s_2 e^{(s_1 + s_2)t} + s_2^2 e^{2s_2 t}] \right\} dt = \frac{v_j^2}{d} \tag{16}$$

As the goal is to minimize W, i.e., the total energy stored in the system, the problem can thus be transformed into maximizing d, as given in Eq. (14).

For a simply supported beam, the normalized modal shape can be expressed as $U_j(x) = \sqrt{2/\rho_b A_b L_b}$ sin $(j\pi x/L_b)$, and the natural frequency is, $\omega_j = j^2\pi^2/L_b^2 \sqrt{E_b J_b/\rho_b A_b}$, where E_b, J_b, ρ_b and A_b are the Young's modulus, moment of inertia, density and cross sectional area of the beam, respectively. Eq. (14) can be rewritten as follows based on the modal shape of the simply supported beam.

$$d = 2\zeta_j \omega_j + S \cdot \sum_{i=1}^{Np} \frac{[\cos(j\pi x_{i2}/L_b) - \cos(j\pi x_{i1}/L_b)]^2}{x_{i2} - x_{i1}} \tag{17}$$

where $$S = -g \cdot b r^a d_{31} E_p h_{31} r^s h^s \frac{2}{\rho_b A_b L_b} \frac{j^2\pi^2}{L_b^2}.$$

By differentiating Eq. (17) with respect to x_{i1} and x_{i2} respectively, the maximization of Eq. (17) is equivalent to solving the following equations.

$$\begin{cases} L_b\cos(j\pi x_{i1}/L_b) - L_b\cos(j\pi x_{i2}/L_b) + 2j\pi(x_{i1} - x_{i2})\sin(j\pi x_{i1}/L_b) = 0 \\ L_b\cos(j\pi x_{i1}/L_b) - L_b\cos(j\pi x_{i2}/L_b) + 2j\pi(x_{i1} - x_{i2})\sin(j\pi x_{i2}/L_b) = 0 \end{cases}, (i = 1,2,...,Np) \tag{18}$$

For a simply supported cylindrical shell, substituting the modal shape functions $U_{pq}(x, \beta) = \sin(p\pi x/L)\sin(q\pi\beta/\beta^*)$ into Eqs. (6) and (7), Eq. (14) can be expressed as

$$d = 2\zeta_j \omega_j + T \cdot \sum_{i=1}^{Np} \frac{[\cos(p\pi x_{i1}/L) - \cos(p\pi x_{i2}/L)]^2}{x_{i2} - x_{i1}} \cdot \frac{[\cos(q\pi\beta_{i1}/\beta^*) - \cos(q\pi\beta_{i2}/\beta^*)]^2}{\beta_{i2} - \beta_{i1}} \tag{19}$$

where $$T = g \cdot \frac{4e_{31}^a}{\rho h} \cdot \frac{h^s e_{31}^s}{R\varepsilon_{33}} \left\{ \frac{1}{pq\pi^2 R} + r^a \left[\frac{p}{qL^2} + \frac{q}{p(R\beta^*)^2} \right] \right\} \cdot \left[\frac{\beta^* L}{pq\pi^2} + r^s \left(\frac{p}{q} \frac{R\beta^*}{L} + \frac{q}{p} \frac{L}{R\beta^*} \right) \right].$$

By differentiating Eq. (19) with respect to x_{i1}, x_{i2}, β_{i1} and β_{i2}, respectively, the maximization of Eq. (19) is equivalent to solving the following equations.

$$\begin{cases} L\cos(p\pi x_{i1}/L) - L\cos(p\pi x_{i2}/L) + 2p\pi(x_{i1}-x_{i2})\sin(p\pi x_{i1}/L) = 0 \\ L\cos(p\pi x_{i1}/L) - L\cos(p\pi x_{i2}/L) + 2p\pi(x_{i1}-x_{i2})\sin(p\pi x_{i2}/L) = 0 \\ \beta^*\cos(q\pi\beta_{i1}/\beta^*) - \beta^*\cos(q\pi\beta_{i2}/\beta^*) + 2q\pi(\beta_{i1}-\beta_{i2})\sin(q\pi\beta_{i1}/\beta^*) = 0 \\ \beta^*\cos(q\pi\beta_{i1}/\beta^*) - \beta^*\cos(q\pi\beta_{i2}/\beta^*) + 2q\pi(\beta_{i1}-\beta_{i2})\sin(q\pi\beta_{i2}/\beta^*) = 0 \end{cases}, (i = 1,2,...,Np) \quad (20)$$

If the solutions of Eqs. (18) and (20) satisfy the constraints given in Eq. (12), the optimal geometric distributions of the piezoelectric S/As are the solutions of Eqs. (18) and (20). Otherwise, if there is conflict between the solutions and the constraints, the SQP method is employed with the help of the optimization functions provided in MATLAB which are based on the standard optimization algorithms. In constrained optimization, the general aim is to transform the problem into an easier sub-problem that can then be solved and used as the basis of an iterative process. The SQP method represents state-of-the-art in nonlinear programming. The method allows one to closely mimic Newton's method for constrained optimization just as is done for unconstrained optimization. At each major iteration, an approximation is made of the Hessian of the Lagrangian function using a quasi-Newton updating method. This is then used to generate a quadratic programming (QP) sub-problem whose solution is used to form a search direction for a line search procedure.

4. Semi-analytical solutions for combined vibration modes

Assuming the first N vibration modes are considered simultaneously when Np pieces of piezoelectric S/As are used, the close-loop vibration equation with negative velocity feedback considered can be written as

$$\dot{\chi} = \boldsymbol{A}\chi \quad (21)$$

where $\boldsymbol{A}$ is as given in Eq. (11), and can be rewritten as follows with the design variables included if the feedback gain matrix is set as a constant g.

$$\boldsymbol{A} = \begin{bmatrix} \mathbf{0}_{N\times N} & & \boldsymbol{I}_{N\times N} & & \\ & d_{11} & d_{12} & & d_{1N} \\ -\boldsymbol{\Omega}^2 & d_{21} & d_{22} & \cdots & d_{2N} \\ & \vdots & \vdots & & \vdots \\ & d_{N1} & d_{N2} & & d_{NN} \end{bmatrix} \quad (22)$$

where for simply supported beam

$$d_{jk} = -2\zeta_j\omega_j\delta_{jk} - S\cdot\sum_{i=1}^{Np}\frac{[\cos(j\pi x_{i2}/L_b) - \cos(j\pi x_{i1}/L_b)]\cdot[\cos(k\pi x_{i2}/L_b) - \cos(k\pi x_{i1}/L_b)]}{x_{i2}-x_{i1}} \quad (23)$$

$$(j = 1,2,\cdots,N, k = 1,2,\cdots,N),$$

and S is as given in Eq. (17); and for simply supported cylindrical shell

$$d_{jk} = -2\zeta_j \omega_j \delta_{jk} - T \cdot \sum_{i=1}^{Np} \frac{[\cos(p\pi x_{i1}/L) - \cos(p\pi x_{i2}/L)] \cdot [\cos(r\pi x_{i1}/L) - \cos(r\pi x_{i2}/L)]}{x_{i2} - x_{i1}} \cdot \frac{[\cos(q\pi\beta_{i1}/\beta^*) - \cos(q\pi\beta_{i2}/\beta^*)] \cdot [\cos(s\pi\beta_{i1}/\beta^*) - \cos(s\pi\beta_{i2}/\beta^*)]}{\beta_{i2} - \beta_{i1}} \tag{24}$$

$$(j = n\cdot(p-1)+q,\ p = 1,2,\cdots,m, q = 1,2,\cdots,n,\ k = n\cdot(r-1)+s,\ r = 1,2,\cdots,m, s = 1,2,\cdots,n)$$

and T is as given in Eq. (19).

Note that in Eqs. (23) and (24), $\delta_{jk} = 1$ ($j = k$) and $\delta_{jk} = 0$ ($j \neq k$).

If $N = 2$, by solving the Lyapunov equation given in Eq. (11) and substituting the solution $\boldsymbol{P}$ into Eq. (10), the total energy W stored in the system can be obtained as follows by assuming the initial condition $\chi(0) = [0\ \ 0\ \ v_1\ \ v_2]^T$.

$$W = -\{(d_{11}\omega_2^2 + d_{22}\omega_1^2)(d_{11} + d_{22})[d_{22}v_1^2 + v_2(-2d_{12}v_1 + d_{11}v_2)] + (d_{22}v_1^2 + d_{11}v_2^2)(\omega_1^2 - \omega_2^2)^2\} / \{d_{22}\omega_1^2[d_{11}^2 d_{22} - d_{12}^2 d_{22} + d_{11}(-d_{12}^2 + d_{22}^2 + \omega_1^2)] + d_{11}[d_{11}^2 d_{22} + d_{11}(-d_{12}^2 + d_{22}^2) - d_{22}(d_{12}^2 + 2\omega_1^2)]\omega_2^2 + d_{11}d_{22}\omega_2^4\} \tag{25}$$

Note that if $d_{12} = 0$ and $v_2 = 0$ are assumed, which means that the second vibration mode is ignored, Eq. (25) can be simplified as $-v_1^2/d_{11}$, which is identical with Eq. (16) in which the first vibration mode is considered.

For the case $N = 3$ and assuming that the initial condition is $\chi(0) = [0\ \ 0\ \ 0\ \ v_1\ \ v_2\ \ v_3]^T$, the total energy can be derived as Eq. (A1) presented in the appendix.

If $d_{13} = 0$, $d_{23} = 0$ and $v_3 = 0$ are assumed and substituted into Eq. (A1), which implies that only the first two vibration modes are considered, Eq. (A1) can be simplified as follows

$$W = -(\alpha(d_{11}r_1 + d_{22})(d_{11} + d_{22})(d_{22}v_1^2 + v_2(-2d_{12}v_1 + d_{11}v_2)) + (d_{22}v_1^2 + d_{11}v_2^2)(1 - r_1)^2\alpha^2) / (d_{22}\alpha(d_{11}^2 d_{22} - d_{12}^2 d_{22} + d_{11}(-d_{12}^2 + d_{22}^2 + \alpha)) + d_{11}(d_{11}^2 d_{22} + d_{11}(-d_{12}^2 + d_{22}^2) - d_{22}(d_{12}^2 + 2\alpha))r_1\alpha + d_{11}d_{22}r_1^2\alpha^2)$$

which is identical with Eq. (25) that is for the first two combined modes if $\omega_1^2 = \alpha$ and $\omega_2^2 = r_1\omega_1^2$ are substituted into Eq. (25).

For the combined vibration modes, although the objective function can be explicitly derived with design variables included, as shown in Eqs. (25) and (A1), the expressions are quite complicated and it is difficult to obtain the corresponding derivatives for the design variables. Thus, the SQP method is employed for the optimization of the combined vibration modes.

5. Results and discussions

In this section, based on the analytical expression of the total energy stored in the system and the

analytical solution for the case of single vibration mode, three examples of a simply supported beam, a simply supported cylindrical shell and a simply supported plate are presented to illustrate the feasibility and efficiency of the analytical and semi-analytical methods for optimal vibration control.

5.1 Simply supported beam

Consider a simply supported beam with collocated S/As bonded on its surfaces, as shown in Fig. 1. The characteristic data of the beam are listed in Table 1. In the following design, the first four vibration modes are assumed to be the controlled modes, which are considered either separately or simultaneously. The initial conditions of the generalized coordinate vector are given by Yang *et al.* (2005) as

$$\eta(0)^T = [0\ 0\ 0\ 0] \text{ and } \dot{\eta}(0)^T = [0.2\ 0.4\ 0.6\ 0.8]$$

to ensure the first four vibration modes are roughly equivalent to the kinetic energy stored in the uncontrolled system.

In order to ensure the system is asymptotically stable, the feedback control gain matrix $\boldsymbol{G}$ is set as a constant of 0.4.

5.1.1 Analytical optimization solution for single vibration mode

Optimization of the distributions of the S/As for single vibration mode can be obtained from Eq. (18) if the jth vibration mode for Np pieces of S/As are considered. For those not satisfying the design

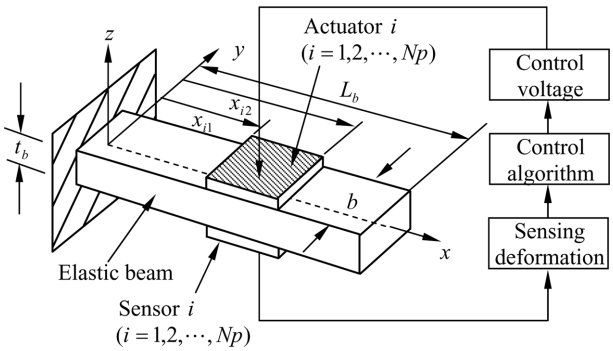

Fig. 1 Beam model with sensors and actuators

Table 1 Beam and piezoelectric patch specifications

Item	Beam	Actuators	Sensors
Mass density (kg/m^3)	1190	1800	1800
Young's modulus (GPa)	3.1028	2	2
Poisson's ration	0.3	0.3	0.3
Piezo-constant d_{31} (m/V)		2.3×10^{-11}	2.3×10^{-11}
Piezo-constant h_{31} (V/m)			4.32×10^{8}
Thickness (m)	1.6×10^{-3}	4×10^{-5}	4×10^{-5}
Length (m)	0.5		
Width (m)	0.01		
Damping ratio	0.01		

Table 2 Optimal placement and size of S/As for single vibration mode of simply supported beam

*j*th mode / patch *Np*	1st		2nd		3rd		4th	
	x_{i1}~x_{i2} (m)	*W*	x_{i1}~x_{i2} (m)	*W*	x_{i1}~x_{i2} (m)	*W*	x_{i1}~x_{i2} (m)	*W*
1	0.0645-0.4355	0.0533	0.2822-0.4678	0.0439	0.1882-0.3118	0.0373	0.3911-0.4839	0.0324
1*	0.0645-0.4355	0.0533	0.2822-0.4678	0.0439	0.1882-0.3118	0.0373	0.1411-0.2339	0.0324
2	0.0681-0.3915	0.0530	0.0322-0.2177	0.0324	0.0215-0.1452	0.0257	0.2661-0.3589	0.0213
	0.3915-0.4655		0.2822-0.4678		0.1882-0.3118		0.3911-0.4839	
2*	0.0678-0.3966	0.0530	0.0322-0.2178	0.0324	0.0215-0.1452	0.0257	0.0161-0.1088	0.0213
	0.3966-0.4670		0.2822-0.4678		0.3548-0.4785		0.2661-0.3588	
3	0.0372-0.1183	0.0527	0.0323-0.2177	0.0322	0.0215-0.1452	0.0196	0.1411-0.2339	0.0158
	0.1183-0.3813		0.2841-0.4458		0.1882-0.3117		0.2611-0.3589	
	0.3813-0.4624		0.4458-0.4828		0.3548-0.4785		0.3911-0.4839	
3*	0.0375-0.1190	0.0527	0.0322-0.2178	0.0322	0.0215-0.1452	0.0196	0.0161-0.1088	0.0158
	0.1190-0.3814		0.2834-0.4547		0.1882-0.3118		0.1411-0.2338	
	0.3814-0.4626		0.4547-0.4854		0.3548-0.4785		0.3911-0.4839	
4	0.0386-0.1213	0.0526	0.0323-0.2178	0.0319	0.0217-0.1452	0.0195	0.0161-0.1089	0.0126
	0.1213-0.3613		0.2683-0.3090		0.1880-0.3116		0.1411-0.2339	
	0.3613-0.4230		0.3090-0.4408		0.3559-0.4631		0.2661-0.3589	
	0.4230-0.4785		0.4408-0.4813		0.4631-0.4885		0.3912-0.4839	
4*	0.0280-0.0864	0.0526	0.0334-0.2046	0.0320	0.0227-0.1305	0.0195	0.0161-0.1089	0.0126
	0.0864-0.1553		0.2046-0.2353		0.1305-0.1552		0.1411-0.2339	
	0.1553-0.3769		0.2674-0.3046		0.1882-0.3118		0.2661-0.3589	
	0.3769-0.4613		0.3046-0.4659		0.3548-0.4785		0.3911-0.4839	
5	0.0264-0.0817	0.0525	0.0326-0.1908	0.0317	0.0213-0.1452	0.0193	0.0158-0.1091	0.0125
	0.0817-0.1420		0.1908-0.2303		0.1882-0.3117		0.1412-0.2336	
	0.1420-0.3508		0.2684-0.3110		0.3465-0.3752		0.2662-0.3587	
	0.3508-0.4172		0.3110-0.4373		0.3752-0.4581		0.3920-0.4724	
	0.4172-0.4731		0.4373-0.4803		0.4581-0.4870		0.4724-0.4912	
5*	0.0258-0.0794	0.0525	0.0189-0.6000	0.0317	0.0132-0.0421	0.0194	0.0161-0.1089	0.0126
	0.0794-0.1407		0.6000-0.1907		0.0421-0.1437		0.1354-0.1583	
	0.1407-0.3765		0.1907-0.2313		0.1782-0.2028		0.1583-0.2327	
	0.3765-0.4298		0.2673-0.3043		0.2028-0.3106		0.2661-0.3589	
	0.4298-0.4770		0.3043-0.4659		0.3548-0.4785		0.3911-0.4839	

The results marked with * are from Yang *et al*. (2005) using GA method.

constraints given in Eq. (12), the SQP optimization method is employed based on the derived system energy given in Eq. (16). In this case, the *j*th ($j = 1,2,3,4$) vibration mode with one to five pieces of S/As respectively is studied. The obtained optimal geometric distributions of the piezoelectric patches are shown in Table 2 together with the solutions obtained using GA method. It is apparent from Table 2 that the results are in good agreement with those obtained using the GA method. In addition, the objective function values are actually slightly better than those obtained by the GA method, e.g., for the case of the 2nd vibration mode with four pieces of piezoelectric patches and the case of the 4th vibration mode with five pieces of piezoelectric patches. However, the distributions of the piezoelectric patches have some discrepancy for certain cases like the 3rd vibration mode with two pieces of piezoelectric patches. Regardless of the distribution difference, the objective function values are exactly the same which implies that both the results are the optimum. The distribution difference indicates that the optimal solution for this problem is not unique.

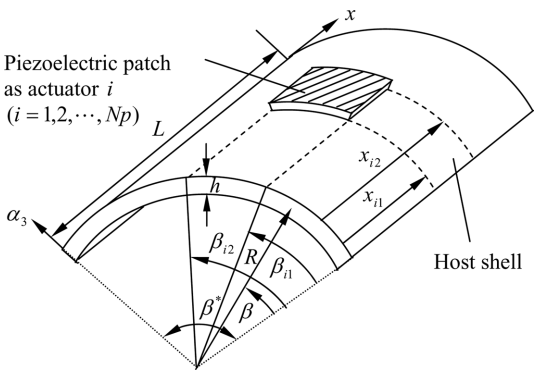

Fig. 2 Thin cylindrical shell with discretely distributed piezoelectric patches

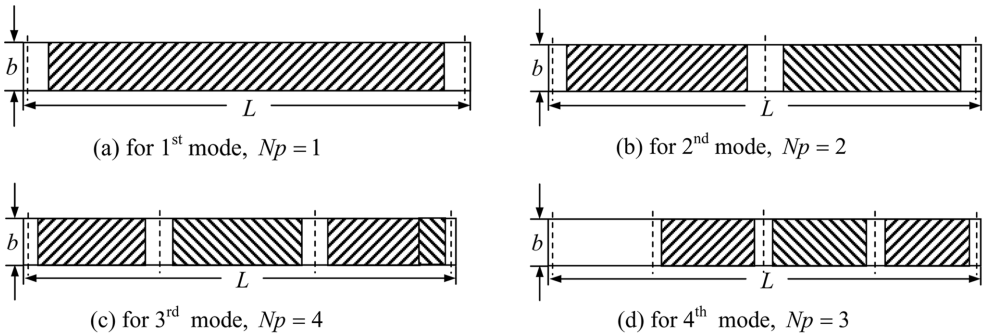

Fig. 3 Optimal geometric distributions of piezoelectric patches for single vibration mode of simply supported beam

The results shown in Table 2 are selectively and schematically depicted in Fig. 3. The dashed lines denote the nodal lines of the vibration modes and the regions filled with diagonal lines represent the piezoelectric patches bonded on the beam, to intuitively show the geometric distributions of the S/As. The figure is drawn diversely for the cases where the piezoelectric patch numbers are more or less the same as the number of regions separated by the vibration nodal lines. It can be seen from Fig. 3 that for the single vibration mode, no matter how many piezoelectric patches are used, the optimal distributions of the piezoelectric patches should be located within the regions separated by the vibration nodal lines. This finding agrees with the conclusion drawn by Yang *et al.* (2005).

It was found that for the cases where the number of piezoelectric patches is less than or equal to the number of regions separated by the corresponding vibration nodal lines, the results can always be obtained from the solutions of Eq. (18). For other cases, the use of the SQP method is necessary.

5.1.2 Semi-analytical optimization solutions for combined vibration modes

For this case, the first few vibration modes are considered simultaneously, i.e., the first two and the first three vibration modes with one to seven pieces of piezoelectric patches are addressed respectively. As explained in the previous section, for the optimization of combined vibration modes, the SQP method is employed based on the analytical expression of the objective function. The obtained optimal geometric distributions of the piezoelectric patches are shown in Table 3 together with the solutions obtained using the GA method. It can be seen from Table 3 that the computed objective function values are identical with those obtained by the GA method. Moreover, both the geometric distributions of the

Table 3 Optimal placement and size of S/As for combined vibration modes of simply supported beam

N modes / patch *Np*	1st and 2nd		1st and 2nd [*]		1st, 2nd and 3rd		1st, 2nd and 3rd [*]	
	x_{i1}~x_{i2} (m)	*W*	x_{i1}~x_{i2} (m)	*W*	x_{i1}~x_{i2} (m)	*W*	x_{i1}~x_{i2} (m)	*W*
1	0.0349-0.2442	0.1049	0.0349-0.2442	0.1049	0.0245-0.1730	0.1500	0.0245-0.1730	0.1500
2	0.0364-0.2500	0.0873	0.0364-0.2500	0.0873	0.0251-0.1797	0.1238	0.0251-0.1797	0.1238
	0.2500-0.4636		0.2500-0.4636		0.3203-0.4749		0.3203-0.4749	
3	0.0381-0.2136	0.0857	0.0381-0.2137	0.0857	0.0275-0.1807	0.1090	0.0275-0.1810	0.1090
	0.2136-0.2864		0.2137-0.2865		0.1807-0.3194		0.1810-0.3206	
	0.2864-0.4619		0.2865-0.4619		0.3194-0.4725		0.3206-0.4724	
4	0.0383-0.1936	0.0852	0.0384-0.1937	0.0852	0.0278-0.1663	0.1066	0.0278-0.1663	0.1066
	0.1936-0.2499		0.1937-0.2500		0.1663-0.2490		0.1663-0.2490	
	0.2499-0.3062		0.2500-0.3063		0.2490-0.3333		0.2490-0.3332	
	0.3062-0.4618		0.3063-0.4616		0.3333-0.4722		0.3332-0.4722	
5	0.0222-0.0712	0.0848	0.0222-0.0717	0.0848	0.0283-0.1511	0.1052	0.0283-0.1511	0.1052
	0.0712-0.1942		0.0717-0.1944		0.1511-0.2093		0.1511-0.2094	
	0.1942-0.2502		0.1944-0.2505		0.2093-0.2907		0.2094-0.2907	
	0.2502-0.3062		0.2505-0.3067		0.2907-0.3490		0.2907-0.3491	
	0.3062-0.4615		0.3067-0.4616		0.3490-0.4717		0.3491-0.4717	
6	0.0223-0.0719	0.0844	0.0223-0.0717	0.0844	0.0283-0.1411	0.1046	0.0283-0.1415	0.1046
	0.0719-0.1941		0.0717-0.1941		0.1411-0.1910		0.1415-0.1914	
	0.1941-0.2500		0.1941-0.2500		0.1910-0.2489		0.1914-0.2496	
	0.2500-0.3059		0.2500-0.3059		0.2489-0.3080		0.2496-0.3083	
	0.3059-0.4283		0.3059-0.4283		0.3080-0.3585		0.3083-0.3584	
	0.4283-0.4778		0.4283-0.4778		0.3585-0.4717		0.3584-0.4717	
7	--	--	--	--	0.0171-0.0563	0.1041	0.0172-0.0560	0.1041
					0.0563-0.1447		0.0560-0.1449	
					0.1447-0.1941		0.1449-0.1945	
					0.1941-0.2532		0.1945-0.2540	
					0.2532-0.3098		0.2540-0.3104	
					0.3098-0.3591		0.3104-0.3597	
					0.3591-0.4714		0.3597-0.4718	

The results marked with [*] are from Yang *et al*. (2005) using GA method.

piezoelectric patches coincide, with minor differences in the order of fourth decimal digit for some cases. This is different from the case of single vibration mode which has different distributions of piezoelectric patches but with identical objective function values because of the multi-solutions of the problem.

Some selected results of Table 3 are schematically shown in Fig. 4 for better illustration of the geometric distributions of the piezoelectric patches. It can be seen from Fig. 4 that unlike for the single vibration mode, for some cases, the distributions of the piezoelectric patches are not located within the regions separated by the nodal lines of the combined vibration modes. In conjunction with Fig. 4 and with further observation from Table 3, it can be found that when the number of piezoelectric patches used is identical with the number of regions separated by the nodal lines of the combined vibration modes, the optimal distributions of the patches should be located within these regions. However, for other numbers of patches used, it may not be tenable. This result is the same as concluded by Yang *et al.* (2005) using the GA method.

For the SQP method, the final optimization results highly depend on the initial point chosen for the

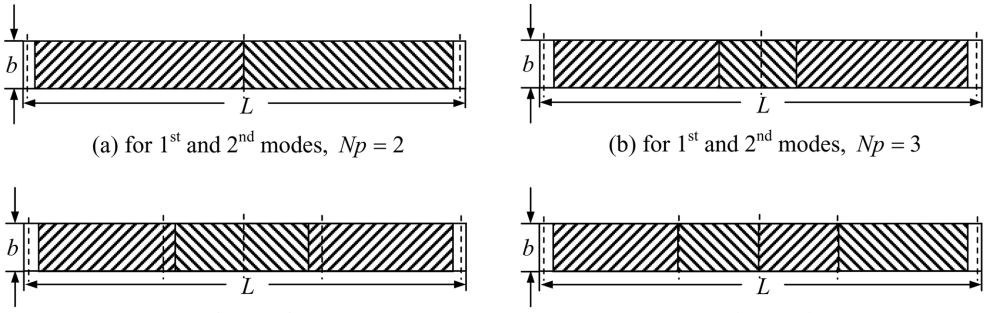

Fig. 4 Optimal geometric distributions of piezoelectric patches for combined vibration modes of simply supported beam

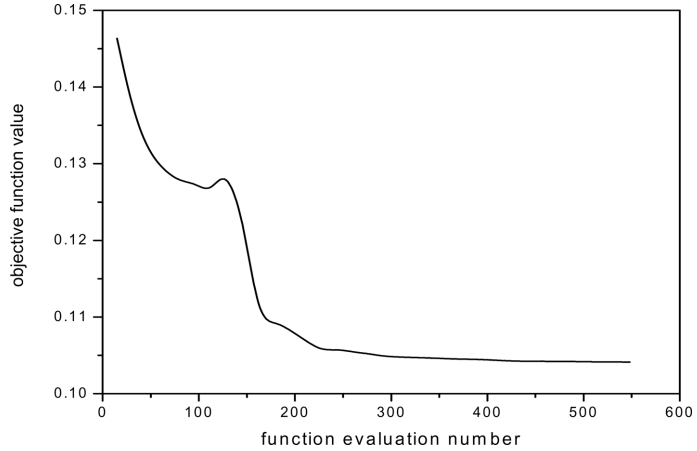

Fig. 5 Objective function value history versus function evaluation number for a typical case

optimization process as local optimum may be obtained if the initial point is not appropriately chosen. From the computation for the case of the first three vibration modes, it is found that the final optimization results can be achieved for an average of 6 times out of the 100 randomly generated initial points used. It means that for the other 94 initial points, the local optimum is obtained or the optimization process failed because of exceeding the preset function evaluation or iteration numbers. For the GA method, there is no guaranty that the global optimum for each optimization process can be found either. If a good initial population is chosen, there is a possibility of finding a better result with even faster speed for the GA method.

To check the efficiency of the proposed method in terms of the number of function evaluation within the iteration processes, a more complicated case of the first three vibration modes with 7 piezoelectric patches used is studied. The objective function value versus the number of function evaluation is shown in Fig. 5. It can be seen that the final result is obtained with about 600 times of function evaluation. Actually a maximum of 1400 times of function evaluation was set as the termination criterion in the simulation, which implies that the final optimum can be obtained with at most 1400 times of function evaluation.

In Yang *et al*. (2005), the GA control parameters like the population size and the maximum number of generations were set at 200 and 300, respectively. A maximum approximated number of 200×300=

Table 4 Cylindrical shell and piezoelectric patch specifications

Item	Shell	Actuators	Sensors
Mass density (kg/m^2)	7800	7600	1780
Young's modulus (GPa)	210	1.6	1.6
Poisson's ration	0.3	0.3	0.3
Piezo-constant d_{31} (m/V)		6×10^{-12}	30×10^{-12}
Piezo-constant e_{31} (N/(V·m))		0.0096	0.048
Permittivity constant ε_{33} (F/m)			8.85×10^{-9}
Thickness (m)	0.001	0.0004	0.0004
Length (m)	1.0		
Curvature angle (rad)	$\pi/3$		
Radius (m)	1.2		
Damping ratio	0.01		

60,000 was used for the function evaluation to obtain the final optimum, which is significantly larger than the number used in the proposed method. This means the proposed method is much more efficient than the GA method from the computation point of view.

5.2 Simply supported cylindrical shell

Consider a cylindrical shell with four edges simply supported on which collocated S/As are bonded, as shown in Fig. 2. The material properties and dimensions of the system are listed in Table 4. The first six ($m = 2$, $n = 3$) vibration modes with initial conditions of $\eta(0)^T$ = [0 0 0 0 0 0] and $\dot{\eta}(0)^T$ = [0.5 0.4 0.3 0.2 0.2 0.1] are investigated either separately or with some modes combined. The feedback control gain matrix is set as a constant of 10.0.

5.2.1 Analytical optimization solution for single vibration mode

To investigate the optimal geometric distributions of the S/As for single vibration mode, the jth ($j = n\cdot(p\text{-}1)+q$) vibration mode with one to five pieces of S/As is separately investigated. Three cases of p=1 and q=2, p=2 and q=2, and p=1 and q=3 are addressed with the obtained optimal geometric distributions of the piezoelectric patches shown in Table 5. Similar to the case of the simply supported beam, Eq. (20) was used to obtain the results for the above mentioned three cases with the number of piezoelectric patches less than or equal to 2, 4 and 3, respectively. If more piezoelectric patches were used, the SQP method was employed for the optimization due to the violation of constraints as presented in Eq. (12). Actually the numbers shown above for different vibration modes are the numbers of regions separated by the nodal lines of the individual vibration mode.

Some results of Table 5 are selectively illustrated in Fig. 6. From Fig. 6 and Table 5, it is apparent that for single vibration mode, the optimal distributions of piezoelectric patches should be located within the regions separated by the nodal lines regardless of the number of patches used. This finding is the same as concluded from the example of the simply supported beam.

5.2.2 Semi-analytical optimization solutions for combined vibration modes

As the analytical expression of the total energy stored in the system is derived up to N=3 vibration modes, the first two and first three vibration modes are addressed separately, i.e., m=1 and n=2, m=2 and n=1, and m=1 and n=3. The same number of patches as adopted by Jin *et al*. (2005) for these three

Table 5 Optimal placement and size of S/As for single vibration mode of simply supported cylindrical shell

*j*th mode / patch *Np*	$p=1, q=2$		$p=2, q=2$		$p=1, q=3$	
	x_{i1}~x_{i2} (m), β_{i1}~β_{i2}(rad)	W (10^{-3})	x_{i1}~x_{i2} (m), β_{i1}~β_{i2}(rad)	W (10^{-3})	x_{i1}~x_{i2} (m), β_{i1}~β_{i2}(rad)	W (10^{-3})
1	0.1290-0.8710, 0.5911-0.9797	4.9211	0.0645-0.4355, 0.5911-0.9797	0.7017	0.1290-0.8710, 0.7432-1.0022	4.7761
2	0.1290-0.8710, 0.0675-0.4561 0.1290-0.8710, 0.5911-0.9797	3.9145	0.5645-0.9355, 0.0675-0.4561 0.0645-0.4355, 0.5911-0.9797	0.6515	0.1290-0.8710, 0.3941-0.6531 0.1290-0.8710, 0.7432-1.0022	3.6429
3	0.1290-0.8710, 0.0713-0.4100 0.1290-0.8710, 0.4100-0.4874 0.1290-0.8710, 0.5911-0.9797	3.8945	0.5645-0.9355, 0.0675-0.4561 0.0645-0.4355, 0.5911-0.9797 0.0645-0.4355, 0.0675-0.4561	0.6081	0.1290-0.8710, 0.0450-0.3040 0.1290-0.8710, 0.3941-0.6531 0.1290-0.8710, 0.7432-1.0022	2.9443
4	0.1290-0.8710, 0.0713-0.4100 0.1290-0.8710, 0.4100-0.4874 0.1290-0.8710, 0.5598-0.6372 0.1290-0.8710, 0.6372-0.9759	3.8747	0.0645-0.4355, 0.5911-0.9797 0.0645-0.4355, 0.0675-0.4561 0.5645-0.9355, 0.0675-0.4561 0.5645-0.9355, 0.5911-0.9797	0.5701	0.1290-0.8710, 0.0241-0.0758 0.1290-0.8710, 0.0758-0.3015 0.1290-0.8710, 0.3941-0.6531 0.1290-0.8710, 0.7432-1.0022	2.9302
5	0.1290-0.8710, 0.0713-0.4100 0.1290-0.8710, 0.4100-0.4874 0.1290-0.8710, 0.5627-0.6477 0.1290-0.8710, 0.6477-0.9231 0.1290-0.8710, 0.9231-1.0081	3.8509	0.0645-0.4355, 0.5911-0.9797 0.0645-0.4355, 0.0675-0.4561 0.5645-0.9355, 0.0675-0.4561 0.5645-0.9355, 0.5598-0.6372 0.5645-0.9355, 0.6372-0.9759	0.5692	0.1290-0.8710, 0.0475-0.2733 0.1290-0.8710, 0.2733-0.3250 0.1290-0.8710, 0.3966-0.6224 0.1290-0.8710, 0.6224-0.6740 0.1290-0.8710, 0.7432-1.0022	2.9162

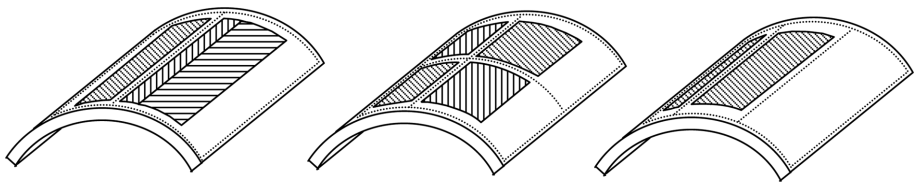

(a) p=1, q=2, Np=3 (b) p=2, q=2, Np=4 (c) p=1, q=3, Np=2

Fig. 6 Optimal geometric distributions of piezoelectric patches for single vibration mode of simply supported cylindrical shell

different cases is used for the purpose of comparison. The optimal geometric distributions of the piezoelectric patches are shown in Table 6 together with the solutions obtained using the GA method. It can be seen from Table 6 that for the first two cases, both methods attained identical objective function values with minor difference in the geometric distributions. However, for the third case, a better

Table 6 Optimal placement and size of S/As for combined vibration modes of simply supported cylindrical shell

$m = 1$, $n = 2$		$m = 2$, $n = 1$		$m = 1$, $n = 3$	
x_{i1}~x_{i2} (m), β_{i1}~β_{i2}(rad)	W (10^{-3})	x_{i1}~x_{i2} (m), β_{i1}~β_{i2}(rad)	W (10^{-3})	x_{i1}~x_{i2} (m), β_{i1}~β_{i2}(rad)	W (10^{-2})
0.1290-0.8710, 0.0741-0.5221 0.1290-0.8710, 0.5252-0.9731	7.7511	0.0967-0.5005, 0.1351-0.9121 0.5005-0.9031, 0.1351-0.9121	5.4831	0.1290-0.8710, 0.0557-0.3400 0.1290-0.8710, 0.3400-0.4955 0.1290-0.8710, 0.4955-0.6920 0.1290-0.8710, 0.6920-0.9920	1.0719
Results below are from Jin *et al.* (2005) using GA method.					
0.1290-0.8710, 0.0741-0.5221 0.1290-0.8710, 0.5252-0.9731	7.7511	0.0992-0.5000, 0.1351-0.9121 0.5000-0.9009, 0.1351-0.9121	5.4831	0.1290-0.8715, 0.0787-0.3564 0.1290-0.8715, 0.3564-0.5585 0.1290-0.8715, 0.5585-0.7303 0.1290-0.8715, 0.7303-0.9722	1.0929

objective function value is obtained by the proposed method, which implies that the proposed method is more effective in achieving better solutions. In the work of Jin *et al*. (2005), the correctness and effectiveness of the GA method was validated by comparing with the work of Sadri *et al*. (1999). The agreement between the results obtained by the proposed method with those obtained by Jin *et al*. (2005) shows the correctness and effectiveness of the proposed method in this paper.

In addition to effectiveness, efficiency of the proposed method is quite salient when comparing the number of function evaluations for both methods. Similar study as for the simply supported beam has been done and it was found that the number of function evaluations required for the proposed method to obtain the optimum is significantly less than that for the GA method, which provides the advantage of reducing computation efforts without compromising accuracy of results.

5.3 Simply supported plate

Assuming $R \to \infty$ and $y = R \cdot \beta$, the simply supported cylindrical shell can be converted into a plate with four edges simply supported. In this section, a simply supported plate with material properties and system dimensions shown in Table 7 is studied. Similar to the simply supported cylindrical shell, the first six ($m = 2$, $m = 3$) vibration modes with the same initial conditions are investigated. The feedback control gain matrix is set as a constant of 10.0 as well.

5.3.1 Analytical optimization solution for single vibration mode

Substituting $R \to \infty$ and $y = R \cdot \beta$ into Eqs. (19) and (20), Eq. (19) can be simplified as

$$d = 2\zeta_j \omega_j + T \cdot \sum_{i=1}^{Np} \frac{[\cos(p\pi x_{i1}/L) - \cos(p\pi x_{i2}/L)]^2}{x_{i2} - x_{i1}} \cdot \frac{[\cos(q\pi y_{i1}/a) - \cos(q\pi y_{i2}/a)]^2}{y_{i2} - y_{i1}} \quad (26)$$

Table 7 Plate and piezoelectric patch specifications

Item	Plate	Actuators	Sensors
Mass density (kg/m^3)	7800	7600	1780
Young's modulus (GPa)	210	63	2
Poisson's ration	0.3	0.3	0.3
Piezo-constant d_{31} (m/V)		37×10^{-12}	30×10^{-12}
Piezo-constant e_{31} (N/(V·m))		2.331	0.06
Permittivity constant ε_{33} (F/m)			8.85×10^{-9}
Thickness (m)	0.001	0.0004	0.0004
Length L (m)	1.0		
Width a (m)	2.0		
Damping ratio	0.01		

where $T = g \cdot \dfrac{4e_{31}^a}{\rho h} \cdot \dfrac{h^s e_{31}^s}{\varepsilon_{33}} r^a r^s aL\left(\dfrac{p}{qL^2} + \dfrac{q}{pa^2}\right)^2$ and a is the width of the plate, and Eq. (20) can be simplified as

$$\begin{cases} L\cos(p\pi x_{i1}/L) - L\cos(p\pi x_{i2}/L) + 2p\pi(x_{i1} - x_{i2})\sin(p\pi x_{i1}/L) = 0 \\ L\cos(p\pi x_{i1}/L) - L\cos(p\pi x_{i2}/L) + 2p\pi(x_{i1} - x_{i2})\sin(p\pi x_{i2}/L) = 0 \\ a\cos(q\pi y_{i1}/a) - a\cos(q\pi y_{i2}/a) + 2q\pi(y_{i1} - y_{i2})\sin(q\pi y_{i1}/a) = 0 \\ a\cos(q\pi y_{i1}/a) - a\cos(q\pi y_{i2}/a) + 2q\pi(y_{i1} - y_{i2})\sin(q\pi y_{i2}/a) = 0 \end{cases}, (i = 1,2,...,Np) \quad (27)$$

Eq. (27) can be used to obtain the solutions for the single vibration mode if no constraint presented in Eq. (12) is violated, otherwise it is necessary to use the SQP method to obtain the solutions. Similar to the simply supported cylindrical shell, three cases of $p = 1$ and $q = 2$, $p = 2$ and $q = 2$, and $p = 1$ and $q = 3$ are addressed and the obtained optimal geometric distributions of the piezoelectric patches are shown in Table 8. Fig. 7 graphically shows the geometric distributions of the piezoelectric patches based on some selected results from Table 8. It can be seen from Table 8 and Fig. 7 that, the optimal distributions of piezoelectric patches should be located within the regions separated by the nodal lines of the single vibration mode is still applicable.

5.3.2 Semi-analytical optimization solutions for combined vibration modes

Substituting $R\to\infty$ and $y = R\cdot\beta$ into Eq. (24), the coefficients in the expression of the total energy stored in the system can be simplified as

$$d_{jk} = -2\zeta_j\omega_j\delta_{jk} - T\cdot\sum_{i=1}^{Np}\frac{[\cos(p\pi x_{i1}/L) - \cos(p\pi x_{i2}/L)]\cdot[\cos(r\pi x_{i1}/L) - \cos(r\pi x_{i2}/L)]}{x_{i2} - x_{i1}}\cdot$$

$$\frac{[\cos(q\pi y_{i1}/a) - \cos(q\pi y_{i2}/a)]\cdot[\cos(s\pi y_{i1}/a) - \cos(s\pi y_{i2}/a)]}{y_{i2} - y_{i1}}$$

$$(j = n\cdot(p-1) + q,\ p = 1,2,\cdots,m, q = 1,2,\cdots,n,\ k = n\cdot(r-1) + s,\ r = 1,2,\cdots,m, s = 1,2,\cdots,n) \quad (28)$$

where T is as given in Eq. (26).

Similar to the simply supported cylindrical shell, the first two and the first three vibration modes are investigated respectively, with the same numbers of piezoelectric patches as those of Yang *et al*. (2006).

Table 8 Optimal placement and size of S/As for single vibration mode of simply supported plate

*j*th mode / patch *Np*	$p=1, q=2$		$p=2, q=2$		$p=1, q=3$	
	x_{i1}~x_{i2} (m), y_{i1}~y_{i2} (m)	W	x_{i1}~x_{i2} (m), y_{i1}~y_{i2} (m)	W (10^{-2})	x_{i1}~x_{i2} (m), y_{i1}~y_{i2} (m)	W (10^{-2})
1	0.1290-0.8710, 0.1290-0.8710	0.1242	0.0645-0.4355, 1.1290-1.8710	1.1051	0.1290-0.8710, 0.7527-1.2473	4.1342
2	0.1290-0.8710, 0.1290-0.8710 0.1290-0.8710, 1.1290-1.8710	0.0818	0.5645-0.9355, 0.1290-0.8710 0.5645-0.9355, 1.1290-1.8710	0.7031	0.1290-0.8710, 0.0860-0.5807 0.1290-0.8710, 1.4193-1.9140	2.6893
3	0.1290-0.8710, 0.1290-0.8710 0.1290-0.8710, 1.1362-1.7830 0.1290-0.8710, 1.7830-1.9309	0.0811	0.5645-0.9355, 0.1290-0.8710 0.0645-0.4355, 1.1290-1.8710 0.0645-0.4355, 0.1290-0.8710	0.5155	0.1290-0.8710, 0.0860-0.5807 0.1290-0.8710, 0.7527-1.2473 0.1290-0.8710, 1.4193-1.9140	1.9928
4	0.1290-0.8710, 0.0691-0.2170 0.1290-0.8710, 0.2170-0.8640 0.1290-0.8710, 1.1362-1.7830 0.1290-0.8710, 1.7830-1.9309	0.0804	0.5645-0.9355, 0.1290-0.8710 0.5645-0.9355, 1.1290-1.8710 0.0645-0.4355, 1.1290-1.8710 0.0645-0.4355, 0.1290-0.8710	0.4070	0.1290-0.8710, 0.0860-0.5807 0.1290-0.8710, 0.7575-1.1886 0.1290-0.8710, 1.1886-1.2873 0.1290-0.8710, 1.4193-1.9140	1.9799
5	0.1290-0.8710, 0.1362-0.7829 0.1290-0.8710, 0.7829-0.9309 0.1290-0.8710, 1.0747-1.2370 0.1290-0.8710, 1.2370-1.7629 0.1290-0.8710, 1.7629-1.9251	0.0796	0.5645-0.9355, 0.1290-0.8710 0.5645-0.9355, 1.1290-1.8710 0.0645-0.4355, 1.1290-1.8710 0.0645-0.4355, 0.0691-0.2170 0.0645-0.4355, 0.2170-0.8640	0.4048	0.1290-0.8710, 0.0860-0.5807 0.1290-0.8710, 0.7527-1.2473 0.1290-0.8710, 1.3832-1.4913 0.1290-0.8710, 1.4913-1.8420 0.1290-0.8710, 1.8420-1.9502	1.9646

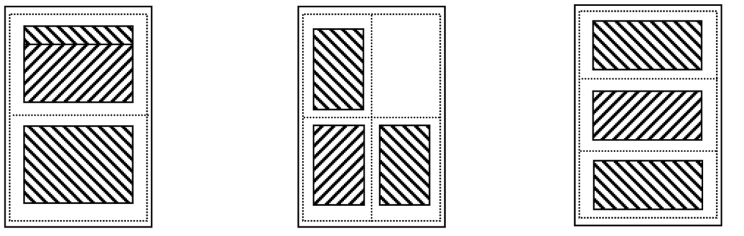

(a) m=1, n=2, Np=3 (b) m=2, n=2, Np=3 (c) m=1, n=3, Np=3

Fig. 7 Optimal geometric distributions of piezoelectric patches for single vibration mode of simply supported plate

The obtained optimal geometric distributions of the piezoelectric patches are shown in Table 9 together with the solutions obtained using the GA method. It can be seen from Table 9 that the objective function values are more or less the same though some discrepancy exists in the geometric distributions

Table 9 Optimal placement and size of S/As for combined vibration modes of simply supported plate

$m = 1, n = 2$		$m = 2, n = 1$		$m = 1, n = 3$	
x_{i1}~x_{i2} (m), y_{i1}~y_{i2} (m)	W	x_{i1}~x_{i2} (m), y_{i1}~y_{i2} (m)	W	x_{i1}~x_{i2} (m), y_{i1}~y_{i2} (m)	W
0.1290-0.8710, 0.1913-1.0024 0.1290-0.8710, 1.0024-1.8080	0.3624	0.1129-0.5006, 0.2580-1.7420 0.5006-0.8870, 0.2580-1.7420	0.2982	0.1290-0.8710, 0.1467-0.6440 0.1290-0.8710, 0.6440-0.9973 0.1290-0.8710, 0.9973-1.3560 0.1290-0.8710, 1.3560-1.8524	0.3720
Results below are from Yang *et al*. (2006) using GA method.					
0.1290-0.8710, 0.1919-1.0141 0.1290-0.8710, 1.0141-1.8087	0.3625	0.1130-0.5017, 0.2580-1.7420 0.5017-0.8871, 0.2580-1.7420	0.2982	0.1290-0.8710, 0.1503-0.6807 0.1290-0.8710, 0.6807-1.0667 0.1290-0.8710, 1.0667-1.3948 0.1290-0.8710, 1.3948-1.8568	0.3722

of the piezoelectric patches. However, slightly better results are obtained by the proposed method in terms of the objective function values.

Again, similar study for the efficiency of the proposed method has been conducted. That less number of function evaluations is required for the proposed method to find the optimum demonstrates that the proposed method is more efficient than the GA method.

6. Conclusions

In this paper, the optimal design of the vibration control system for smart structures was studied. The placements and sizes of the piezoelectric S/As were optimized based on the energy dissipation criteria. The total energy stored in the system, used as the objective function, was analytically derived for the optimization. For the case of single vibration mode, the optimal result could be analytically obtained by differentiating the objective function. Those conflicting with the constraints were solved using the SQP method, which was also applied to the combined vibration mode case with quite complicated expression of objective function. The results of a simply supported beam, a simply supported cylindrical shell and a simply supported plate agreed well with those obtained by GA, and were even slightly better for the objective function values for some cases. Similar conclusions about the relationship of the distributions of the piezoelectric S/As and specific vibration modes were drawn in comparison with the GA method. More importantly, it was found that the proposed method was much more efficient than the GA method with regard to the optimization process time. The proposed method provides an alternate counterpart for the optimal vibration control of smart structures, in a more efficient way. With the modification of objective function, it can be easily extended to other applications such as plates and shells.

References

Arockiasamy, M., Neelakanta, P.S. and Sreenivasan, G. (1992), "Vibration control of beams with embedded smart composite material", *J. Aerospace Eng.*, **5**(4), 492-498.

Bailey, T. and Hubbard, Jr. J.E. (1985), "Distributed piezoelectric-polymer active vibration control of a cantilever beam", *J. Guid. Control Dynam.*, **8**(5), 605-611.

Baz, A. and Poh, S. (1988), "Performance of an active control system with piezoelectric actuators", *J. Sound Vib.*, **126**(2), 327-343.

Bruant, I., Coffignal, G., Lene, F. and Verge, M. (2001), "A methodology for determination of piezoelectric actuator and sensor location on beam structures", *J. Sound Vib.*, **243**(5), 861-882.

Chandrashekhara, K. and Agarwal, A.N. (1993), "Active vibration control of laminated composite plates using piezoelectric devices: a finite element approach", *J. Intel. Mat. Syst. Str.*, **4**(4), 496-508.

Crawley, E.F. and de Luis, J. (1987), "Use of piezoelectric actuators as elements of intelligent structures", *AIAA J.*, **25**(10), 1373-1385.

Devasia, S., Meressi, T., Paden, B. and Bayo, E. (1993), "Piezoelectric actuator design for vibration suppression: placement and sizing", *J. Guid. Control Dynam.*, **16**(5), 859-864.

Jin, Z.L., Yang, Y.W. and Soh, C.K. (2005), "Application of fuzzy GA for optimal vibration control of smart cylindrical shells", *Smart Mater. Struct.*, **14**(6), 1250-1264.

Kalaycioglu, S., Giray, M. and Asmer, H. (1998), "Vibration control of flexible manipulators using smart structures", *J. Aerospace Eng.*, **11**(3), 90-94.

Kondoh, S., Yatomi, C. and Inoue, K. (1990), "The positioning of sensors and actuators in the vibration control of flexible systems", *JSME Int. J.*, **33**(2), 145-152.

Krishnakumar, K. and Goldberg, D.E. (1992), "Control system optimization using genetic algorithms", *J. Guid. Control Dynam.*, **15**(3), 735-740.

Lee, A.C. and Chen, S.T. (1994), "Collocated sensor/actuator positioning and feedback design in the control of flexible structure system", *J. Vib. Acoust.*, **116**(2), 146-154.

Lee, I. and Han, J.H. (1996), "Optimal placement of piezoelectric actuators in intelligent structures using genetic algorithms", *Proceedings of the 3rd International Conference on Intelligent Materials and 3rd European Conference on Smart Structures and Materials*, Lyon, France, June.

Qing, G., Qiu, J. and Liu, Y. (2006), "A semi-analytical solution for static and dynamic analysis of plates with piezoelectric patches", *Int. J. Solids Struct.*, **43**(6), 1388-1403.

Sadri, A.M., Wright, J.R. and Wynne, R.J. (1999), "Modelling and optimal placement of piezoelectric actuators in isotropic plates using genetic algorithms", *Smart Mater. Struct.*, **8**(4), 490-498.

Udwadia, F.E. (1994), "Methodology for optimum sensor locations for parameter identification in dynamic systems", *J. Eng. Mech.-ASCE*, **120**(2), 368-390.

Varadan, V.V., Kim, J. and Varadan, V.K. (1997), "Optimal placement of piezoelectric actuators for active noise control", *AIAA J.*, **35**(3), 526-533.

Wang, Q. and Quek, S.T. (2002), "A model for the analysis of beams with embedded piezoelectric layers", *J. Intel. Mat. Syst. Str.*, **13**(1), 61-70.

Yang, Y.W., Jin, Z.L. and Soh, C.K. (2005), "Integrated optimal design of vibration control system for smart beams using genetic algorithms", *J. Sound Vib.,* **282**(3-5)**,** 1293-1307.

Yang, Y.W., Jin, Z.L. and Soh, C.K. (2006), "Integrated optimization of control system for smart cylindrical shells using modified GA", *J. Aerospace Eng.*, **19**(2), 68-79.

Yang, Y.W., Ju, C.K. and Soh, C.K. (2003), "Analytical and semi-analytical solutions for vibration control of a cantilevered column using a piezoelectric actuator", *Smart Mater. Struct.*, **12**(2), 193-203.

Zhang, H.W., Lennox, B., Goulding, P.R. and Leung, A.Y.T. (2000), "A float-encoded genetic algorithm technique for integrated optimization of piezoelectric actuator and sensor placement and feedback gains", *Smart Mater. Struct.*, **9**, 552-557.

CC

Appendix

$$W = -(v_1^2 P_1 + v_2^2 P_2 + v_3^2 P_3 + \frac{v_1 v_2}{d_{12}}(1 - d_{11}P_1 - d_{22}P_2 + d_{33}P_3) + \frac{v_1 v_3}{d_{13}}(1 - d_{11}P_1 + d_{22}P_2 - d_{33}P_3) + \frac{v_2 v_3}{d_{23}}(1 + d_{11}P_1 - d_{22}P_2 - d_{33}P_3)) \tag{A1}$$

where, $P_1 = P_{1\ell}/P$, $P_2 = P_{2\ell}/P$, $P_3 = P_{3\ell}/P$, and

$$P_{1\ell} = (d_{23}^2 - d_{22}d_{33})(d_{12}^2 d_{22} + 2d_{12}d_{13}d_{23} + d_{13}^2 d_{33} - d_{11}^2(d_{22} + d_{33}) - (d_{22} + d_{33})(-d_{23}^2 + d_{22}d_{33}) + d_{11}(d_{12}^2 + d_{13}^2 - (d_{22} + d_{33})^2))(d_{33}r_1(d_{23}^2 + d_{13}^2 r_1 - d_{33}(d_{22} + d_{11}r_1)) + (-d_{22}^2 d_{33} + d_{22}(d_{23}^2 - 2d_{11}d_{33}r_1) + r_1(2d_{12}d_{13}d_{23} + d_{11}(d_{13}^2 - d_{11}d_{33})r_1))r_2 + (d_{12}^2 - d_{11}d_{22})(d_{22} + d_{11}r_1)r_2^2) - \alpha(d_{22}^5 \cdot d_{33}(-1 + r_2)^2 r_2 - 2d_{12}d_{13}^3 d_{23}r_1(-1 + r_2)(d_{33}r_1(-1 + r_2) - d_{22}(-1 + r_1)r_2) + d_{11}^3 d_{22}d_{33}(r_1 - r_2)^2 \cdot (d_{22}(1 + r_1)r_2 + d_{33}r_1(1 + r_2)) + d_{22}^4(-1 + r_2)^2(-d_{23}^2 r_2 + d_{33}^2(r_1 + r_2)) - d_{23}^2 d_{33}^2(-1 + r_1)r_1(d_{33}^2 \cdot (-1 + r_1) + 2d_{23}^2(-1 + r_2) - d_{12}^2(-1 + r_2^2)) + d_{22}^3 d_{33}(-2d_{12}^2(r_1 - r_2)(-1 + r_2)r_2 + d_{23}^2(r_1 - r_2) \cdot (-1 + r_2^2) + d_{33}^2(r_1(1 + r_1) + r_2 + (-6 + r_1)r_1 r_2 + (1 + r_1)r_2^2)) + d_{22}^2(-2d_{23}^4(-1 + r_1)(-1 + r_2) \cdot r_2 + d_{23}^2 d_{33}^2(r_1 - 4r_1^2 + r_2 + r_1(4 + r_1)r_2 + (-4 + r_1)r_2^2) + d_{33}^2(-1 + r_1)^2(-d_{12}^2 r_2(1 + r_2) + d_{33}^2 \cdot (r_1 + r_2))) + d_{22}d_{33}(d_{12}^4(-1 + r_1)^2 r_2^2 + r_1(d_{33}^4(-1 + r_1)^2 + d_{13}^4 r_1(-1 + r_2)^2 + d_{11}^4(r_1 - r_2)^2 r_2) - d_{12}^2 d_{33}^2(-1 + r_1)^2(r_1 + r_2^2) + d_{23}^2(-d_{33}^2(-1 + r_1^2)(r_1 - r_2) + d_{12}^2(-1 + r_2)^2(r_1^2 + r_2)) + d_{23}^4(r_1^2(3 - 2r_2) + r_2(-2 + 3r_2) - 2r_1(1 + (-1 + r_2)r_2))) + (-d_{23}^2 d_{33}^2(-1 + r_1)^2 r_1(-1 + r_2)^2 + d_{22}^3 d_{33}(-1 + r_2)^2(r_1^2 + r_2 + (-4 + r_1)r_1 r_2 + r_2^2) + d_{22}^2(-1 + r_1)^2(-1 + r_2)^2(-d_{23}^2 r_2 + d_{33}^2(r_1 + r_2)) + d_{22}d_{33} \cdot (-1 + r_1)(-d_{23}^2(-1 + r_2)(r_1^2(-3 + r_2) + r_2 - 3r_2^2 + r_1(1 + r_2)^2) + (-1 + r_1)(-2d_{12}^2(r_1 - r_2)(-1 + r_2)r_2 + d_{33}^2(r_1^2 + r_2^2 + r_1(1 + (-4 + r_2)r_2))))\alpha + d_{22}d_{33}(-1 + r_1)^2(r_1 - r_2)^2(-1 + r_2)^2\alpha^2 - d_{13}^2(d_{22}^3 d_{33}(-1 + r_2)^2(r_1^2 + r_2) + d_{22}^2(-1 + r_2)(d_{33}^2 r_1(1 + r_1)(-1 + r_2) + d_{23}^2 r_2 + d_{11}d_{33}r_1(-1 + r_2)(r_1 + r_2) + r_2(-(d_{12}^2 + d_{23}^2)r_1^2 + d_{12}^2 r_2)) + r_1(d_{11}^2 d_{12}^2(r_1 - r_2)^2 r_2 + d_{11}d_{33}(-2d_{23}^2 r_1(-1 + r_2)^2 + d_{12}^2(r_1 - r_2)^2(1 + r_2)) + d_{12}^2(-1 + r_1)(4d_{23}^2(-1 + r_2)r_2 + d_{33}^2(r_1 - r_2^2))) + d_{22}(-2d_{11}^2 d_{33}(-1 + r_1)r_1(r_1 - r_2)r_2 - d_{23}^2(-1 + r_1)^2(d_{11}r_2(r_1 + r_2) + d_{33}(r_1 + r_2^2)) + d_{11}(d_{12}^2(1 + r_1)(r_1 - r_2)^2 r_2 - 2d_{33}^2 r_1(r_2 + r_2^2 + r_1^2(1 + r_2) - 2r_1(1 + r_2^2))) + d_{33}(r_1 - r_2)(-2d_{33}^2(-1 + r_1)r_1 + d_{12}^2(r_1 - r_2)(r_1 + r_2) - 2(-1 + r_1)r_1(-1 + r_2)^2\alpha))) + d_{11}(d_{22}^4 d_{33}(1 + r_1)(-1 + r_2)^2 r_2 + d_{23}^2 d_{33}r_1(-d_{33}^2(-1 + r_1)^2 \cdot (1 + r_2) + d_{12}^2(-1 + r_2)^2(r_1 + r_2)) + d_{22}^3(-d_{23}^2(1 + r_1)(-1 + r_2)^2 r_2 + d_{33}^2(r_1(1 + r_2)(1 + (-6 + r_2)r_2) + 2r_1^2(1 + r_2^2) + 2(r_2 + r_2^3))) + d_{22}^2 d_{33}(2d_{12}^2 r_2(r_1(1 + r_1) - 2(1 + r_1^2)r_2 + (1 + r_1)r_2^2) + d_{33}^2 \cdot (2r_1(1 + r_1^2) + (1 + r_1)(1 + (-6 + r_1)r_1)r_2 + 2(1 + r_1^2)r_2^2) - d_{23}^2(r_1(1 + r_2)(1 + (-6 + r_2)r_2) + 2r_1^2 \cdot (1 + r_2^2) + 2(r_2 + r_2^3)) + (1 + r_1)(r_1 - r_2)^2(-1 + r_2)^2\alpha) + d_{22}(d_{23}^2(2d_{12}^2(-1 + r_1)^2 r_2^2 - d_{33}^2(2r_1 \cdot (1 + r_1^2) + (1 + r_1)(1 + (-6 + r_1)r_1)r_2 + 2(1 + r_1^2)r_2^2)) + d_{33}^2(-1 + r_1)^2(d_{33}^2 r_1(1 + r_2) - d_{12}^2 r_2(r_1 +$$

$$r_2)+(r_1-r_2)^2(1+r_2)\alpha)))+d_{11}^2(d_{22}^3d_{33}r_2(r_1(1+r_1)+r_2+(-6+r_1)r_1r_2+(1+r_1)r_2^2)-d_{23}^2\cdot d_{33}^2r_1(r_2+r_1(1+r_2(-4+r_1+r_2)))+d_{22}^2(d_{33}^2(r_1^2(2-5r_2)+r_2^2(2+r_2)+r_1r_2^2(-5+2r_2)+r_1^3(1+2r_2))-d_{23}^2r_2(r_2+r_1(1+r_2(-4+r_1+r_2))))+d_{22}d_{33}(d_{33}^2r_1(r_1(1+r_1)+r_2+(-6+r_1)\cdot r_1r_2+(1+r_1)r_2^2)-2d_{23}^2(r_1^2(1-2r_2)+r_1^3r_2+r_2^2+r_1(-2+r_2)r_2^2)+(r_1-r_2)(-2d_{12}^2r_1(-1+r_2)r_2+(r_1-r_2)(r_2+r_1(1+r_2(-4+r_1+r_2)))\alpha)))+2d_{12}d_{13}d_{23}(d_{22}^2(1+r_1)(d_{33}(-1+r_1)+d_{11}(r_1-r_2))(-1+r_2)r_2+d_{22}^3(r_1-r_2)(-1+r_2)r_2+d_{23}^2(-d_{22}(-1+r_1)r_2(-1+r_1(-2+r_2)+2r_2)-d_{33}r_1(-1+r_2)(-1-2r_2+r_1(2+r_2)))-d_{33}(-1+r_1)r_1(d_{33}^2(r_1-r_2)+d_{11}^2(r_1-r_2)r_2+d_{11}d_{33}(r_1-r_2)(1+r_2)+(-1+r_2)(-d_{12}^2r_2+(r_1-r_2)(-1+r_2)\alpha))+d_{22}(d_{33}^2(-1+r_1)r_1(-1+r_2^2)+r_2(d_{11}^2r_1(r_1-r_2)(-1+r_2)+(-1+r_1)^2(-d_{12}^2r_2+(r_1-r_2)(-1+r_2)\alpha))))) \tag{A2}$$

$$\begin{aligned}P_{2t}=&(d_{13}^2-d_{11}d_{33})(d_{12}^2d_{22}+2d_{12}d_{13}d_{23}+d_{13}^2d_{33}-d_{11}^2(d_{22}+d_{33})-(d_{22}+d_{33})(-d_{23}^2+d_{22}d_{33})+\\&d_{11}(d_{12}^2+d_{13}^2-(d_{22}+d_{33})^2))(d_{33}r_1(d_{23}^2+d_{13}^2r_1-d_{33}(d_{22}+d_{11}r_1))+(-d_{22}^2d_{33}+d_{22}(d_{23}^2-\\&2d_{11}d_{33}r_1)+r_1(2d_{12}d_{13}d_{23}+d_{11}(d_{13}^2-d_{11}d_{33})r_1))r_2+(d_{12}^2-d_{11}d_{22})(d_{22}+d_{11}r_1)r_2^2)-\alpha(2d_{12}^3\cdot\\&d_{13}d_{23}d_{33}(-1+r_1)(r_1-r_2)r_2+d_{11}^5d_{33}r_1(r_1-r_2)^2r_2+d_{11}^4(r_1-r_2)^2(-d_{13}^2r_1r_2+d_{22}d_{33}(1+r_1)\cdot\\&r_2+d_{33}^2r_1(1+r_2))-d_{12}^2(d_{22}^2d_{23}^2(-1+r_2)^2r_2+d_{22}d_{33}(-d_{13}^2(r_1-r_2)^2(1+r_2)+d_{23}^2(-1+r_2)^2\cdot\\&(r_1+r_2))+(-1+r_1)(d_{13}^2d_{33}^2(-r_1^2+r_2^2)+d_{23}^2(4d_{13}^2(r_1-r_2)r_2+d_{33}^2(-r_1+r_2^2))))+d_{11}^3(2d_{12}d_{13}\cdot\\&d_{23}r_1(r_1-r_2)(-1+r_2)r_2-d_{23}^2d_{33}(r_1-r_2)^2(1+r_1r_2)+d_{22}^2d_{33}r_2(r_1(1+r_1)+r_2+(-6+r_1)r_1r_2+\\&(1+r_1)r_2^2)+d_{33}r_1(d_{33}^2(r_1(1+r_1)+r_2+(-6+r_1)r_1r_2+(1+r_1)r_2^2)+(r_1-r_2)(-1+r_2)(-2d_{12}^2\cdot\\&r_2+d_{13}^2(r_1+r_2)))+d_{22}(-d_{13}^2(1+r_1)(r_1-r_2)^2r_2+d_{33}^2(r_1^2(2-5r_2)+r_2^2(2+r_2)+r_1r_2^2(-5+\\&2r_2)+r_1^3(1+2r_2)))+d_{33}(r_1-r_2)^2(r_2+r_1(1+r_2(-4+r_1+r_2)))\alpha)-d_{13}^2d_{33}(d_{22}^2d_{33}(r_1^2+r_2+\\&(-4+r_1)r_1r_2+r_2^2)+d_{22}(-2d_{23}^2(r_1-r_2)^2+d_{33}^2(-1+r_1)^2(r_1+r_2))+d_{33}(-1+r_1)(d_{33}^2(-1+r_1)\cdot\\&r_1+(r_1-r_2)(2d_{13}^2r_1+(-1+r_1)(r_1-r_2)\alpha)))-2d_{12}d_{13}d_{23}d_{33}(d_{33}^2(-1+r_1)r_1(-1+r_2)+d_{22}^2(-1+\\&r_1)(-1+r_2)r_2+d_{22}d_{33}(-1+r_1)(-1+r_2)(r_1+r_2)+(r_1-r_2)(d_{13}^2(-r_2+r_1(-2+r_1+2r_2))+(r_1-\\&r_2)(d_{23}^2+(-1+r_1)(-1+r_2)\alpha)))+d_{11}^2(2d_{12}d_{13}d_{23}d_{33}(-1+r_1)(1+r_1)(r_1-r_2)r_2+d_{22}^3d_{33}(1+r_1)\cdot\\&(-1+r_2)^2r_2+d_{33}^4(-1+r_1)^2r_1(1+r_2)+d_{22}^2(-d_{13}^2r_2(r_1^2+r_2+(-4+r_1)r_1r_2+r_2^2)+d_{23}^2(r_1(1+\\&r_2)(1+(-6+r_2)r_2)+2r_1^2(1+r_2^2)+2(r_2+r_2^3)))+(r_1-r_2)r_2(d_{12}^2d_{23}^2(-1+r_1r_2)+d_{13}^2(-1+r_1)\cdot\\&(-2d_{13}^2r_1+d_{23}^2(1+r_1)-(-1+r_1)(r_1-r_2)\alpha))+d_{22}(2d_{12}d_{13}d_{23}(1+r_1)(r_1-r_2)(-1+r_2)r_2+d_{33}^3\cdot\\&(2r_1(1+r_1^2)+(1+r_1)(1+(-6+r_1)r_1)r_2+2(1+r_1^2)r_2^2)+d_{33}(-d_{23}^2(r_1-r_2)^2(1+r_2)+2d_{12}^2r_2(r_1\cdot\\&(1+r_1)-2(1+r_1^2)r_2+(1+r_1)r_2^2)-d_{13}^2(r_1^2(2-5r_2)+r_2^2(2+r_2)+r_1r_2^2(-5+2r_2)+r_1^3(1+2\cdot\\&r_2))+(1+r_1)(r_1-r_2)^2(-1+r_2)^2\alpha))+d_{33}^2(-d_{23}^2(1+r_1)(r_1-r_2)^2+d_{13}^2r_1(r_2+r_2^2+r_1^2(1+r_2)-\\&4r_1(1+(-1+r_2)r_2))+(-1+r_1)^2(-d_{12}^2r_2(r_1+r_2)+(r_1-r_2)^2(1+r_2)\alpha)))+d_{11}(-2d_{12}^3d_{13}d_{23}(-1+\\&r_1)^2r_2^2+d_{12}^4d_{33}(-1+r_1)^2r_2^2+d_{13}^4d_{33}r_1(-2r_1^2(1+r_2)-2r_2(1+r_2)+r_1(3+r_2(2+3r_2)))+d_{13}^2\cdot\\&(d_{23}^2(-1+r_1)^2(d_{22}r_2(1+r_2)+d_{33}(r_1+r_2^2))-d_{33}(d_{33}^2r_1(-1+r_1^2)(-1+r_2)+d_{22}d_{33}(2(r_1+r_1^3)+\end{aligned}$$

$$
\begin{aligned}
&(1+r_1)(1+(-6+r_1)r_1)r_2+2(1+r_1^2)r_2^2)+2d_{22}^2(r_2+r_2^3-2r_1r_2(1+r_2)+r_1^2(1+r_2^2))+(-1+r_1)\cdot\\
&(r_1-r_2)((-3+r_1)r_1+(1+r_1)^2r_2+(1-3r_1)r_2^2)\alpha))-d_{12}^2(-2d_{13}^2d_{22}(-1+r_1)^2r_2^2+d_{22}d_{33}^2(-1+\\
&r_1)^2r_2(1+r_2)+d_{33}^3(-1+r_1)^2(r_1+r_2^2)+d_{23}^2(-1+r_2)^2(d_{22}(1+r_1)r_2+d_{33}r_1(1+r_2))+d_{33}(r_1-\\
&r_2)(d_{13}^2(-r_1+r_2)(1+r_1r_2)+2(-1+r_2)r_2(d_{22}^2+(-1+r_1)^2\alpha)))+d_{33}(d_{23}^4(r_1-r_2)^2+d_{22}^4(-1+\\
&r_2)^2r_2+d_{22}^3d_{33}(-1+r_2)^2(r_1+r_2)+2d_{23}^2(-1+r_1)(-1+r_2)(d_{33}^2r_1+(r_1-r_2)^2\alpha)+(-1+r_1)^2\cdot\\
&(d_{33}^2r_1+(r_1-r_2)^2\alpha)(d_{33}^2+(-1+r_2)^2\alpha)+d_{22}d_{33}(2d_{23}^2(r_1^2(-2+r_2)+r_2-2r_2^2+r_1(1+r_2^2))+\\
&(-1+r_1)^2(r_1+r_2)(d_{33}^2+(-1+r_2)^2\alpha))+d_{22}^2(d_{33}^2(r_1(1+r_1)+r_2+(-6+r_1)r_1r_2+(1+r_1)r_2^2)+\\
&(-1+r_2)(2d_{23}^2(-1+r_1)r_2+(-1+r_2)(r_1^2+r_2+(-4+r_1)r_1r_2+r_2^2)\alpha)))-2d_{12}d_{13}d_{23}(-d_{33}^2\cdot\\
&(-1+r_1)(r_1-r_2)(r_1+r_2)+r_2(d_{13}^2(-1+r_1)(r_1(2+r_1-2r_2)-r_2)-(r_1-r_2)(d_{22}^2(-1+r_2)+\\
&(-1+r_1)(d_{23}^2+(-1+r_1)(-1+r_2)\alpha))))))
\end{aligned}
\tag{A3}
$$

$$
\begin{aligned}
P_{3t}=\;&(d_{12}^2-d_{11}d_{22})(d_{12}^2d_{22}+2d_{12}d_{13}d_{23}+d_{13}^2d_{33}-d_{11}^2(d_{22}+d_{33})-(d_{22}+d_{33})(-d_{23}^2+d_{22}d_{33})+\\
&d_{11}(d_{12}^2+d_{13}^2-(d_{22}+d_{33})^2))(d_{33}r_1(d_{23}^2+d_{13}^2r_1-d_{33}(d_{22}+d_{11}r_1))+(-d_{22}^2d_{33}+d_{22}(d_{23}^2-\\
&2d_{11}d_{33}r_1)+r_1(2d_{12}d_{13}d_{23}+d_{11}(d_{13}^2-d_{11}d_{33})r_1))r_2+(d_{12}^2-d_{11}d_{22})(d_{22}+d_{11}r_1)r_2^2)-\alpha(-d_{13}^2\cdot\\
&d_{23}^2(d_{33}(-1+r_1)r_1+d_{22}(r_1^2-r_2))(d_{33}(-1+r_1)+d_{22}(-1+r_2))+d_{11}^5d_{22}r_1(r_1-r_2)^2r_2+2d_{12}^4\cdot\\
&d_{22}^2(r_1-r_2)(-1+r_2)r_2+d_{11}^4(r_1-r_2)^2(-d_{12}^2r_1r_2+d_{22}^2(1+r_1)r_2+d_{22}d_{33}r_1(1+r_2))+2d_{12}^3d_{13}d_{22}\cdot\\
&d_{23}(r_1-r_2)((-2+r_2)r_2+r_1(-1+2r_2))-2d_{12}d_{13}d_{22}d_{23}(d_{33}^2(-1+r_1)r_1(-1+r_2)+d_{22}^2(-1+r_1)\cdot\\
&(-1+r_2)r_2+d_{22}d_{33}(-1+r_1)(-1+r_2)(r_1+r_2)+(r_1-r_2)(d_{13}^2r_1(-1+r_2)+(r_1-r_2)(d_{23}^2+(-1+\\
&r_1)(-1+r_2)\alpha)))-d_{12}^2(-d_{22}d_{33}(2d_{23}^2+d_{13}^2(1+r_1))(r_1-r_2)^2-4d_{13}^2d_{23}^2r_1(r_1-r_2)(-1+r_2)+d_{22}^4\cdot\\
&(-1+r_2)^2r_2+d_{22}^3d_{33}(-1+r_2)^2(r_1+r_2)+d_{22}^2(d_{33}^2(r_1^2+r_2^2+r_1(1+(-4+r_2)r_2))+(r_1-r_2)\cdot\\
&(-1+r_2)(d_{13}^2(r_1+r_2)+(r_1-r_2)(-1+r_2)\alpha)))+d_{11}^3(d_{22}^3r_2(r_1(1+r_1)+r_2+(-6+r_1)r_1r_2+(1+\\
&r_1)r_2^2)-d_{12}r_1(r_1-r_2)(2d_{13}d_{23}(-1+r_1)r_2+d_{12}d_{33}(r_1-r_2)(1+r_2))+d_{22}^2d_{33}(r_1^2(2-5r_2)+r_2^2\cdot\\
&(2+r_2)+r_1r_2^2(-5+2r_2)+r_1^3(1+2r_2))+d_{22}(-d_{23}^2(r_1-r_2)^2(1+r_1r_2)+d_{33}^2r_1(r_1(1+r_1)+r_2+\\
&(-6+r_1)r_1r_2+(1+r_1)r_2^2)+(-r_1+r_2)((-1+r_1)r_2(-2d_{13}^2r_1+d_{12}^2(r_1+r_2))+(-r_1+r_2)(r_2+r_1\cdot\\
&(1+r_2(-4+r_1+r_2)))\alpha)))+d_{11}^2(d_{22}^4(1+r_1)(-1+r_2)^2r_2+d_{22}^3d_{33}(r_1(1+r_2)(1+(-6+r_2)r_2)+\\
&2r_1^2(1+r_2^2)+2(r_2+r_2^3))+d_{22}^2(-d_{23}^2r_1^2+d_{12}^2r_1r_2+2d_{23}^2r_1r_2+d_{12}^2r_1^2r_2-d_{23}^2r_1^2r_2-4d_{12}^2r_2^2-\\
&d_{23}^2r_2^2+4d_{12}^2r_1r_2^2+2d_{23}^2r_1r_2^2-4d_{12}^2r_1^2r_2^2+d_{12}^2r_2^3-d_{23}^2r_2^3+d_{12}^2r_1r_2^3-d_{13}^2r_1(-1+r_2)^2(r_1+r_2)+\\
&d_{33}^2(2r_1(1+r_1^2)+(1+r_1)(1+(-6+r_1)r_1)r_2+2(1+r_1^2)r_2^2)+(1+r_1)(r_1-r_2)^2(-1+r_2)^2\alpha)-r_1\cdot\\
&(-2d_{12}^4(r_1-r_2)(-1+r_2)r_2+2d_{12}d_{13}d_{23}d_{33}(-1+r_1)(r_1-r_2)(1+r_2)+d_{13}^2d_{23}^2(r_1-r_2)(-1+r_1\cdot\\
&r_2)+d_{12}^2(d_{23}^2(r_1-r_2)(-1+r_2^2)+d_{33}^2(r_1^2+r_2^2+r_1(1+(-4+r_2)r_2))+(r_1-r_2)^2(-1+r_2)^2\alpha))+\\
&d_{22}(d_{33}^3(-1+r_1)^2r_1(1+r_2)-2d_{12}d_{13}d_{23}r_1(r_1-r_2)(-1+r_2^2)-d_{33}(d_{12}^2(r_1^2(2-5r_2)+r_2^2(2+\\
&r_2)+r_1r_2^2(-5+2r_2)+r_1^3(1+2r_2))-2d_{13}^2r_1(r_2+r_2^2+r_1^2(1+r_2)-2r_1(1+r_2^2))+(r_1-r_2)^2(d_{23}^2\cdot\\
&(1+r_1)-(-1+r_1)^2(1+r_2)\alpha))))+d_{11}(d_{13}^4d_{22}r_1^2(-1+r_2)^2+d_{12}^4d_{22}r_2(-2r_1(1+r_1)+(3+r_1(2+
\end{aligned}
$$

$$
\begin{aligned}
&3r_1))r_2 - 2(1+r_1)r_2^2) + 2d_{12}^3 d_{13} d_{23} r_1(-1+r_2)(r_1 + 2r_1 r_2 - r_2(2+r_2)) - d_{13}^2(d_{22}^2 d_{33} r_1(1+r_1)\cdot \\
&(-1+r_2)^2 + d_{23}^2 d_{33}(-1+r_1)^2 r_1(1+r_2) + d_{22}^3(-1+r_2)^2(r_1^2+r_2) + d_{22}(-1+r_1)(-2d_{33}^2 r_1(r_1 - \\
&r_2) + d_{23}^2(-1+r_1^2)r_2 + 2r_1(-1+r_2)^2(-r_1+r_2)\alpha)) + d_{22}(d_{23}^4(r_1-r_2)^2 + d_{22}^4(-1+r_2)^2 r_2 + d_{22}^3\cdot \\
&d_{33}(-1+r_2)^2(r_1+r_2) + 2d_{23}^2(-1+r_1)(-1+r_2)(d_{33}^2 r_1 + (r_1-r_2)^2\alpha) + (-1+r_1)^2(d_{33}^2 r_1 + \\
&(r_1-r_2)^2\alpha)(d_{33}^2 + (-1+r_2)^2\alpha) + d_{22} d_{33}(2d_{23}^2(r_1^2(-2+r_2) + r_2 - 2r_2^2 + r_1(1+r_2^2)) + \\
&(-1+r_1)^2(r_1+r_2)(d_{33}^2 + (-1+r_2)^2\alpha)) + d_{22}^2(d_{33}^2(r_1(1+r_1) + r_2 + (-6+r_1)r_1 r_2 + (1+r_1)r_2^2) + \\
&(-1+r_2)(2d_{23}^2(-1+r_1)r_2 + (-1+r_2)(r_1^2 + r_2 + (-4+r_1)r_1 r_1 + r_2^2)\alpha))) + d_{12}^2(d_{33} r_1(2d_{13}^2 r_1 + \\
&d_{23}^2(1+r_1))(-1+r_2)^2 - d_{23}^2(-1+r_1)r_2(-1+r_2^2) - d_{22}^2 d_{33}(r_1(1+r_2)(1+(-6+r_2)r_2) + 2r_1^2(1+ \\
&r_2^2) + 2(r_2+r_2^3)) + d_{22}(d_{13}^2(r_1-r_2)^2(1+r_1 r_2) - 2d_{33}^2(r_1 + r_1^3 - 2r_1 r_2 + r_1^2(-2+r_2)r_2 + r_2^2) + \\
&(-1+r_2)(d_{23}^2(-1+r_2)(r_1^2+r_2) - (-r_1+r_2)(r_1^2(1-3r_2) + (-3+r_2)r_2 + r_1(1+r_2)^2)\alpha))) - \\
&2d_{12} d_{13} d_{23}(d_{13}^2 r_1^2(-1+r_2)^2 + (r_1-r_2)(d_{22}^2(-1+r_2)(r_1+r_2) + r_1(d_{23}^2(-1+r_2) + (-1+r_1)\cdot \\
&(d_{33}^2 + (-1+r_2)^2\alpha))))))
\end{aligned}
\tag{A4}
$$

$$
\begin{aligned}
P = &-(d_{13}^2 d_{22} - 2d_{12} d_{13} d_{23} + d_{12}^2 d_{33} + d_{11}(d_{23}^2 - d_{22} d_{33}))(d_{12}^2 d_{22} + 2d_{12} d_{13} d_{23} + d_{13}^2 d_{33} - d_{11}^2\cdot \\
&(d_{22}+d_{33}) - (d_{22}+d_{33})(-d_{23}^2 + d_{22} d_{33}) + d_{11}(d_{12}^2 + (d_{13} - d_{22} - d_{33})(d_{13} + d_{22} + d_{33})))\cdot \\
&(d_{33} r_1(d_{22} d_{33} - d_{13}^2 r_1 + d_{11} d_{33} r_1) - 2d_{12} d_{13} d_{23} r_1 r_2 + (d_{22}^2 d_{33} + 2d_{11} d_{22} d_{33} r_1 + d_{11}(-d_{13}^2 + d_{11}\cdot \\
&d_{33}) r_1^2) r_2 + (-d_{12}^2 + d_{11} d_{22})(d_{22} + d_{11} r_1) r_2^2 - d_{23}^2(d_{33} r_1 + d_{22} r_2)) - (d_{11}^5 d_{22} d_{33} r_1 (r_1 - r_2)^2 r_2 + \\
&2d_{12}^4 d_{22}^2 d_{33}(r_1 - r_2)(-1+r_2) r_2 - 2d_{12}^3 d_{13} d_{22} d_{23}(r_1 - r_2)(d_{22}(-1+r_2) r_2 + d_{33}(r_1 - 2r_1 r_2 - (-2+ \\
&r_2) r_2)) + d_{11}^4(r_1 - r_2)^2(-d_{12}^2 d_{33} r_1 r_2 + d_{22}^2 d_{33}(1+r_1) r_2 + d_{22} r_1(-d_{13}^2 r_2 + d_{33}^2(1+r_2))) + d_{13}^2 d_{33}\cdot \\
&(d_{23}^2 d_{33}^2(-1+r_1)^2 r_1 - d_{22}^3 d_{33}(r_1^2 + r_2 + (-4+r_1) r_1 r_2 + r_2^2) + d_{22}^2(-d_{33}^2(-1+r_1)^2(r_1+r_2) + d_{23}^2\cdot \\
&(r_1^2 + r_2 + (-4+r_1) r_1 r_2 + r_2^2)) + d_{22} d_{33}(-1+r_1)(d_{23}^2(-1+r_1)(r_1+r_2) + r_1(-d_{33}^2(-1+r_1) + 2\cdot \\
&d_{13}^2(-r_1+r_2)))) - 2d_{12} d_{13} d_{23}(-d_{33}^2(-1+r_1) r_1(d_{13}^2(r_1 - r_2) + d_{23}^2(-1+r_2)) + d_{22}^3 d_{33}(-1+r_1)\cdot \\
&(-1+r_2) r_2 + d_{22} d_{33}(d_{33}^2(-1+r_1) r_1(-1+r_2) + d_{13}^2(r_1 - r_2)(-r_2 + r_1(-2+r_1+2r_2)) - d_{23}^2\cdot \\
&(r_1^2(-2+r_2) + r_2 - 2r_2^2 + r_1(1+r_2^2))) + d_{22}^2(d_{23}^2 r_2(-1+r_1+r_2 - r_1 r_2) + d_{33}^2(r_1^2(-2+r_2) + r_2 - \\
&2r_2^2 + r_1(1+r_2^2)))) + d_{12}^2(4d_{13}^2 d_{23}^2 d_{33} r_1(r_1 - r_2)(-1+r_2) - d_{22}^4 d_{33}(-1+r_2)^2 r_2 - d_{22}^3(-1+r_2)^2\cdot \\
&(-d_{23}^2 r_2 + d_{33}^2(r_1+r_2)) + d_{22}^2 d_{33}(d_{23}^2(-1+r_2)^2(r_1+r_2) + 2d_{13}^2(r_1 - r_2)(r_1 - r_2^2) - d_{33}^2(r_1^2 + \\
&r_2^2 + r_1(1+(-4+r_2) r_2))) + d_{22}(2d_{13}^2 d_{33}^2(r_1 - r_2)(r_1^2 - r_2) + d_{23}^2(-4d_{13}^2(-1+r_1)(r_1 - r_2) r_2 + \\
&d_{33}^2(r_1^2 + r_2^2 + r_1(1+(-4+r_2) r_2))))) + d_{11}(d_{12}^4 d_{22} d_{33} r_2(-2r_1(1+r_1) + (3+r_1(2+3r_1)) r_2 - 2\cdot \\
&(1+r_1) r_2^2) + 2d_{12}^3 d_{13} d_{23}(d_{22} r_2(r_1(1+r_1) - 2(1+r_1^2) r_2 + (1+r_1) r_2^2) + d_{33} r_1(-1+r_2)(r_1 + 2r_1\cdot \\
&r_2 - r_2(2+r_2))) + d_{13}^4 d_{22} d_{33} r_1(-2r_1^2(1+r_2) - 2r_2(1+r_2) + r_1(3+r_2(2+3r_2))) + d_{13}^2(d_{23}^2 d_{33}^2\cdot \\
&(-1+r_1)^2 r_1(1+r_2) - 2d_{22}^3 d_{33}(r_2 + r_2^3 - 2r_1 r_2(1+r_2) + r_1^2(1+r_2^2)) + d_{22}^2(2d_{23}^2(-1+r_1) r_2(-1+ \\
&r_1 r_2) - d_{33}^2(2r_1(1+r_1^2) + (1+r_1)(1+(-6+r_1) r_1) r_2 + 2(1+r_1^2) r_2^2)) + d_{22} d_{33}(-1+r_1)(-d_{33}^2\cdot \\
&r_1(1+r_1)(-1+r_2) + d_{23}^2(-1+r_1)(r_2 + 2r_2^2 + r_1(2+r_2)))) + (-d_{23}^2 + d_{22} d_{33})(d_{33}^2(-1+r_1) r_1\cdot \\
&(d_{33}^2(-1+r_1) + 2d_{23}^2(-1+r_2)) + d_{22}^4(-1+r_2)^2 r_2 + d_{22}^3 d_{33}(-1+r_2)^2(r_1+r_2) + d_{22}^2(2d_{23}^2(-1+
\end{aligned}
$$

$$r_1)(-1+r_2)r_2+d_{33}^2(r_1(1+r_1)+r_2+(-6+r_1)r_1r_2+(1+r_1)r_2^2))+d_{22}d_{33}(d_{33}^2(-1+r_1)^2(r_1+$$
$$r_2)+d_{23}^2((2-3r_2)r_2+r_1^2(-3+2r_2)+2r_1(1+(-1+r_2)r_2))))+2d_{12}d_{13}d_{23}(d_{22}^3(r_1-r_2)(-1+$$
$$r_2)r_2+d_{22}^2d_{33}(r_2+r_2^3-2r_1r_2(1+r_2)+r_1^2(1+r_2^2))+d_{22}(-d_{13}^2(-1+r_1)(r_1(2+r_1-2r_2)-r_2)\cdot$$
$$r_2+d_{33}^2(r_1+r_1^3-2r_1r_2+r_1^2(-2+r_2)r_2+r_2^2))-d_{23}^2(d_{22}(-1+r_1)r_2(-1+r_1(-2+r_2)+2r_2)+$$
$$d_{33}r_1(-1+r_2)(-1-2r_2+r_1(2+r_2)))+d_{33}r_1(-d_{33}^2(-1+r_1)(r_1-r_2)+d_{13}^2(r_2+r_2^2+r_1^2(1+$$
$$r_2)-2r_1(1+r_2^2))))+d_{12}^2(-d_{22}^3d_{33}(-1+r_1)r_2(-1+r_2^2)+d_{22}d_{33}(d_{13}^2(r_1-r_2)^2(2+r_1+r_2+2\cdot$$
$$r_1r_2)-2d_{33}^2(r_1+r_1^3-2r_1(1+r_1)r_2+(1+r_1^2)r_2^2)+d_{23}^2(-1+r_2)^2(2r_2+r_1(1+2r_1+r_2)))+r_1\cdot$$
$$(2d_{23}^2(-1+r_2)(-2d_{13}^2(-1+r_1)r_2+d_{33}^2(-1+r_1r_2)+d_{13}^2d_{33}^2(r_1^2+r_2^2+r_1(1+(-4+r_2)r_2)))+$$
$$d_{22}^2(r_2(d_{23}^2(1+r_1)(-1+r_2)^2+d_{13}^2(r_1^2+r_2+(-4+r_1)r_1r_2+r_2^2))-d_{33}^2(r_1(1+r_2)(1+(-6+r_2)\cdot$$
$$r_2)+2r_1^2(1+r_2^2)+2(r_2+r_2^3)))))+d_{11}^3(d_{22}^3d_{33}r_2(r_1(1+r_1)+r_2+(-6+r_1)r_1r_2+(1+r_1)r_2^2)+$$
$$d_{22}(2d_{12}d_{13}d_{23}r_1(r_1-r_2)(-1+r_2)r_2-2d_{23}^2d_{33}(r_1^2(1-2r_2)+r_1^3r_2+r_2^2+r_1(-2+r_2)r_2^2)+d_{33}\cdot$$
$$((r_1-r_2)(r_1+r_2)(d_{13}^2r_1(-1+r_2)-d_{12}^2(-1+r_1)r_2)+d_{33}^2r_1(r_1(1+r_1)+r_2+(-6+r_1)r_1r_2+$$
$$(1+r_1)r_2^2)))-r_1(2d_{12}d_{13}d_{23}d_{33}(-1+r_1)(r_1-r_2)r_2+d_{12}^2(r_1-r_2)^2(-d_{13}^2r_2+d_{33}^2(1+r_2))+d_{23}^2\cdot$$
$$d_{33}^2(r_2+r_1(1+r_2(-4+r_1+r_2))))+d_{22}^2(d_{33}^2(r_1^2(2-5r_2)+r_2^2(2+r_2)+r_1r_2^2(-5+2r_2)+r_1^3\cdot$$
$$(1+2r_2))-r_2(d_{13}^2(1+r_1)(r_1-r_2)^2+d_{23}^2(r_2+r_1(1+r_2(-4+r_1+r_2))))))+d_{11}^2(d_{22}^4d_{33}(1+r_1)\cdot$$
$$(-1+r_2)^2r_2+d_{22}^3(-r_2(d_{23}^2(1+r_1)(-1+r_2)^2+d_{13}^2(r_1^2+r_2+(-4+r_1)r_1r_2+r_2^2))+d_{33}^2(r_1\cdot$$
$$(1+r_2)(1+(-6+r_2)r_2)+2r_1^2(1+r_2^2)+2(r_2+r_2^3)))+d_{22}^2(-2d_{12}d_{13}d_{23}r_2(r_1(1+r_1)-2(1+$$
$$r_1^2)r_2+(1+r_1)r_2^2)-d_{23}^2d_{33}(r_1(1+r_2)(1+(-6+r_2)r_2)+2r_1^2(1+r_2^2)+2(r_2+r_2^3))+d_{33}(d_{12}^2\cdot$$
$$r_2(r_1(1+r_1)-4(1+(-1+r_1)r_1)r_2+(1+r_1)r_2^2)+d_{33}^2(2r_1(1+r_1^2)+(1+r_1)(1+(-6+r_1)r_1)r_2+$$
$$2(1+r_1^2)r_2^2)-d_{13}^2(r_1^2(2-5r_2)+r_2^2(2+r_2)+r_1r_2^2(-5+2r_2)+r_1^3(1+2r_2))))-r_1(d_{12}^2d_{33}\cdot$$
$$(-(r_1-r_2)(2d_{12}^2(-1+r_2)r_2+d_{13}^2(r_1-r_2)(1+r_2))+d_{33}^2(r_1^2+r_2^2+r_1(1+(-4+r_2)r_2)))+2d_{12}\cdot$$
$$d_{13}d_{23}((-d_{13}^2(-1+r_1)+d_{12}^2(-1+r_2))(r_1-r_2)r_2+d_{33}^2(r_2+r_2^2+r_1^2(1+r_2)-2r_1(1+r_2^2)))+$$
$$d_{23}^2d_{33}(d_{33}^2(-1+r_1)^2(1+r_2)+2d_{12}^2(-1+r_2)(r_1-r_2^2)-d_{13}^2(r_2+r_1(1+r_2(-4+r_1+r_2)))))+$$
$$d_{22}(d_{13}^2(-2d_{13}^2(-1+r_1)r_1+d_{12}^2(1+r_1)(r_1-r_2))(r_1-r_2)r_2+d_{33}^4(-1+r_1)^2r_1(1+r_2)+2d_{12}d_{13}\cdot$$
$$d_{23}d_{33}(r_1^2(1-2r_2)+r_1^3r_2+r_2^2+r_1(-2+r_2)r_2^2)+d_{33}^2(-d_{12}^2(r_1^2(2-5r_2)+r_2^2(2+r_2)+r_1r_2^2\cdot$$
$$(-5+2r_2)+r_1^3(1+2r_2))+d_{13}^2r_1(r_2+r_2^2+r_1^2(1+r_2)-4r_1(1+(-1+r_2)r_2)))+d_{23}^2(-d_{33}^2\cdot$$
$$(2r_1(1+r_1^2)+(1+r_1)(1+(-6+r_1)r_1)r_2+2(1+r_1^2)r_2^2)+r_2(2d_{13}^2(-1+r_1)(r_1^2-r_2)+d_{12}^2(r_2+$$
$$r_1(1+r_2(-4+r_1+r_2)))))))\alpha+\alpha^2(d_{22}d_{33}(d_{13}^2d_{33}(-1+r_1)^2+2d_{12}d_{13}d_{23}(-1+r_1)(-1+r_2)+$$
$$d_{12}^2d_{22}(-1+r_2)^2)(r_1-r_2)^2-d_{11}^2(r_1-r_2)^2(-d_{12}^2d_{33}r_1(-1+r_2)^2+d_{22}^2d_{33}(1+r_1)(-1+r_2)^2+$$
$$d_{22}(-1+r_1)^2(-d_{13}^2r_2+d_{33}^2(1+r_2)))-d_{11}^3d_{22}d_{33}(r_1-r_2)^2(r_2+r_1(1+r_2(-4+r_1+r_2)))+d_{11}\cdot$$
$$(d_{23}d_{33}(-1+r_1)r_1(d_{23}d_{33}(-1+r_1)+2d_{12}d_{13}(r_1-r_2))(-1+r_2)^2-d_{22}^3d_{33}(-1+r_2)^2(r_1^2+r_2+$$

$$(-4+r_1)r_1r_2+r_2^2)-d_{22}^2(-1+r_1)^2(-1+r_2)^2(-d_{23}^2r_2+d_{33}^2(r_1+r_2))+d_{22}(-2d_{12}d_{13}d_{23}(-1+r_1)^2(r_1-r_2)(-1+r_2)r_2+d_{23}^2d_{33}(-1+r_1)(-1+r_2)(r_1^2(-3+r_2)+r_2-3r_2^2+r_1(1+r_2)^2)+d_{33}(-d_{33}^2(-1+r_1)^2(r_1^2+r_2^2+r_1(1+(-4+r_2)r_2))+(r_1-r_2)(-d_{12}^2(-1+r_2)(r_1^2(1-3r_2)+(-3+r_2)r_2+r_1(1+r_2)^2+(-1+r_1)(d_{13}^2((-3+r_1)r_1+(1+r_1)^2r_2+(1-3r_1)r_2^2)+(-1+r_1)\cdot(-1+r_2)^2(-r_1+r_2)\alpha))))) \quad \text{(A5)}$$

Note that in Eqs. (A2)-(A5), $\alpha = \omega_1^2$, $r_1 = \omega_2^2/\omega_1^2$, and $r_2 = \omega_3^2/\omega_1^2$.